Electronic Supplementary Material (ESI) for New Journal of Chemistry.

Electronic Supporting Information

Metal-Mediated Generation of Triazapentadienate-terminated Di- and Trinuclear μ_2-Pyrazolate Ni^{II} Species and Control of their Nuclearity

Elena V. Andrusenko, Evgeniy V. Kabin, Alexander S. Novikov, Nadezhda A. Bokach,* Galina L. Starova, Vadim Yu. Kukushkin*

Institute of Chemistry, Saint Petersburg State University, Universitetskaya Nab. 7/9, 199034 Saint Petersburg, Russian Federation

*e-mails: n.bokach@spbu.ru and v.kukushkin@spbu.ru

Table of contents

Nickel(II)-mediated and chelation-driven cascade reaction of $NCNR_2$ and MeOH. The Ni^{II}-mediated integration between cyanamides and alcohols was conducted in the alcohols R'OH (R' = Me, Et, ^{i}Pr). The reactions of $NiX_2 \bullet nH_2O$ and $NCNR_2$ (**Scheme 1**) were attempted at molar ratios in the range between 1:2 and 1:10 and all tests were conducted either at RT or at 50 °C.

We observed that the cascade generation of $(TAP)Ni^{II}$ from $NCNR_2$ proceeds in MeOH on keeping the reaction mixture for two weeks at RT or for 3 d at 50 °C and this reaction gives the complex $[Ni(TAP)_2]$ (**1**; TAP = HN=C(OMe)NC(OMe)=NH; **Scheme 1**, **a**). Compound **1** was isolated as orange crystals after the complete evaporation of the solvent and separation of the residue by column chromatography (yields up to 40%; see later). The reaction observed in MeOH does not proceed when EtOH or ^{i}PrOH were taken as solvents and only generation of the known[1] $(dialkylcyanamide)Ni^{II}$ complexes was detected. Hence, all other experiments were further performed in MeOH.

Although all tested systems involving the cyanamides and Ni^{II} salts gave complex **1**, the best yields of **1** (up to 40%) for the shortest time (2 weeks at RT or 3 d at 50 °C for $R_2 = Me_2$ and $C_2H_4OC_2H_4$; 1 month at RT or 7 d at 50 °C for $R_2 = Et_2$ and C_5H_{10}) were obtained for $NCNR_2$ ($R_2 = Me_2$ and $C_2H_4OC_2H_4$). The highest yield of the product was achieved when a molar ratio between $NiCl_2$ and a cyanamide was in the range between 1:(4–6).

Apart from **1**, several by-products were also identified. The products derived from the methylation of the NR_2 group, viz. $[Me_2NR_2]X$ ($R_2 = Me_2$ and $C_2H_4OC_2H_4$; X = Cl, Br, I), were separated as colorless crystals from the reaction mixtures in MeOH and these salts were identified by $HRESI^+$-MS and, in the case of $[OC_4H_8NMe_2]Cl$, using X-ray diffraction (XRD) by comparison of the obtained crystal lattice parameters with those reported in the literature [space group $P2_12_12_1$; a = 8.2741; b = 9.7521, c = 9.7573 Å; *lit.*[2] space group $P2_12_12_1$; a = 8.2735; b = 9.7455; c = 9.7543 Å]. By contrast to the other alcohols used as solvents in this reaction, in many instances, methanol serves as rather efficient methylation agent, although it is expectedly weaker than, e.g. MeI. In particular, metal-catalyzed methylation of amines with MeOH is the well-known reaction. The

methylation activity of MeOH was reported for both heterogeneous (for recent examples see Refs.[3]) and homogeneous (for recent examples see Refs.[4]) catalytic reactions and it can lead to products exhibiting different degree of the alkylation. We assume that in our systems, MeOH also behaves as the methylation agent toward $NCNR_2$ giving, under nickel(II)-mediated conditions, the ammonia salts, $[Me_2NAlk_2]^+$.

In addition to the ammonium salts, GC-MS analysis allowed the identification of metal-free species originating from nickel(II)-involving methanolysis of $NCNMe_2$, viz. $MeOC(=O)NH_2$ or $MeOC(=O)NMe_2$, and also from hydration of $NCNMe_2$, viz. $NH_2C(=O)NMe_2$. Heterogeneous catalytic hydration of RCN's to amides promoted by nickel centers,[5] and the homogenous hydration with the [(PCP)Ni(OH)] (PCP = bis-2,6-di-alkylphosphinomethylbenzene) complex are known.[6] Complex **1** was separated from by-products by column chromatography on silica gel.

General consideration of the structure of the *bis*-chelate gives an idea that two key steps are required to achieve this compound. Firstly, ammonia should be generated *in situ* from the only nitrogen-containing precursor, $NCNR_2$, by nickel(II)-mediated hydrolysis (**Scheme S1**), whereupon NH_3 undergoes the double coupling with two adjacent nitrile groups (**Scheme S2**) forming a stable 6-membered chelate ring. An example of relevant amine double coupling with two *cis*-ligated nitriles at a rhodium center has been reported by Gunnoe and coworkers.[7] Noteworthy that addition of ammonia (2 equiv) to the $NiCl_2/NCNMe_2$ system in MeOH does not led to increased yield of **1**, and with excess of ammonia generation of **1** is suppressed. This little experiment suggests that the mechanism of the reaction is not simple and it perhaps involves internal generation of ammonia at a nickel(II) center as one of the fast reaction stages.

Secondly, at some stage all NR_2 groups should be replaced with the OMe functionality and this reaction might proceed via substitution of the NR_2 groups in the formed TAP chelates by OMe. Many relevant examples of substitution of NR_2 moieties in urea derivatives with OAlk were documented (for recent works see Refs[8]). The substitution of the NR_2 groups is most likely methylation-assisted as MeOH, in contrast to other alcohols featuring more sterically encumbered

alkyls, is a good alkylation agent. The pronounced ability of MeOH toward alkylation[3b, 9] explains the different behavior of MeOH and the other alcohols in our systems. To summarize, this cascade reaction is Ni^{II}-mediated and chelation-driven. Moreover, MeOH plays the role of alkylation reagent supporting NR_2/OMe replacement in the formed species.

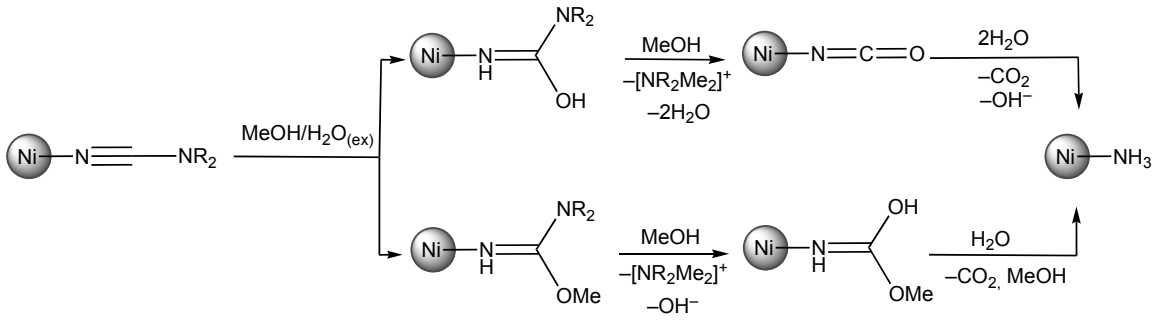

Scheme S1. Postulated mechanism of alkylation-assisted hydrolysis/methanolysis of $NCNR_2$ ligands.

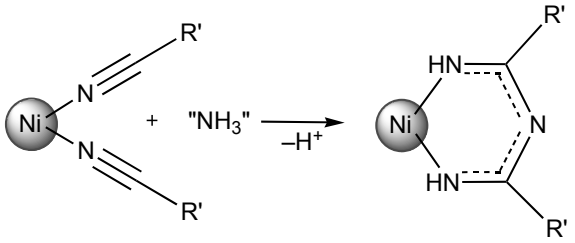

Scheme S2. Schematic representation of the coupling of two Ni^{II}-bonded nitrile species with *in situ* generated NH_3.

Complex **1** was characterized by C, H, and N elemental analyses, high resolution ESI-MS, FTIR, ^{1}H and $^{13}C\{^{1}H\}$ NMR spectroscopies, TG-DTA, and also by single-crystal XRD. The complex gives satisfactory C, H, N, and Ni elemental analyses for the proposed formula. The $HRESI^{+}$ mass-spectrum display a group of peaks corresponding to $[M + H]^{+}$. In the IR spectrum, the 1,3,5-triazapentadienate species exhibit weak narrow double bands at 3364–3344 cm^{-1}, which can be attributed to the N−H stretches. The spectra also display two strong absorption bands at 1614

and 1214 cm^{-1} assigned to ν(C=N) and ν(C–N) of the TAP ligand, respectively. The MeO groups give a strong band at 1394 cm^{-1} from ν(C–O).

In the ^{1}H and $^{13}C\{^{1}H\}$ NMR spectra, the signal of the OMe group appears at 3.58 ppm and at *ca*. 54 ppm, correspondingly. The characteristic feature of the $^{13}C\{^{1}H\}$ NMR spectrum is the presence of the resonance at 163 ppm from C=N of the TAP ligand. Heating of **1** leads to sublimation of the complex at 175 °C (Supporting Information, **Figure S28**).

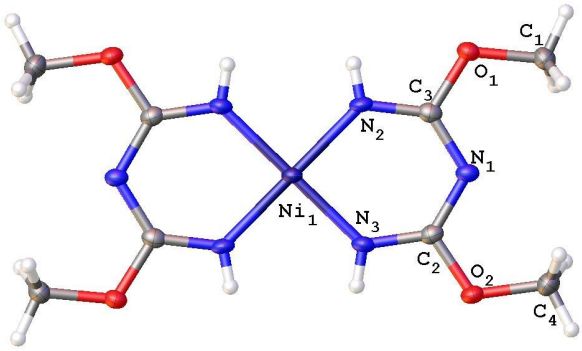

Figure S1. View of the molecular structure of **1**. Thermal ellipsoids are given at the 50% probability level. Selected bond lengths (Å) and angles (°): Ni1–N2 1.8652(16), Ni1–N3 1.8659(16), N3–C2 1.306(2), N2–C3 1.302(2), N1–C2 1.330(2), N1–C3 1.337(2), O1–C3 1.359(2), O1–C1 1.443(2), O2–C2 1.367(2), O2–C4 1.442(2), N2–Ni1–N3 89.66(8), C3–N2–Ni1 127.56(14), C2–N3–Ni1 127.48(14), N2–C3–N1 128.51(18), N3–C2–N1 128.52(17), C2–N1–C3 118.02(17), C3–O1–C1 116.86(14), C2–O2–C4 116.33(15), N3–C2–O2 115.74(16), N2–C3–O1 115.47(16), N1–C2–O2 115.73(16), N1–C3–O1 116.01(16).

The single-crystal XRD data for **1** (**Figure S1**) indicate that the nickel atom has a square-planar environment formed with four N atoms of the two TAP ligands. In the crystal structure, the molecules form the crossed stacks (**Figure S2**) and the shortest nickel•••nickel separation is 5.7496(3) Å (the double Bondi's vdW radius for Ni is 3.26 Å) with no metallophilic interactions.

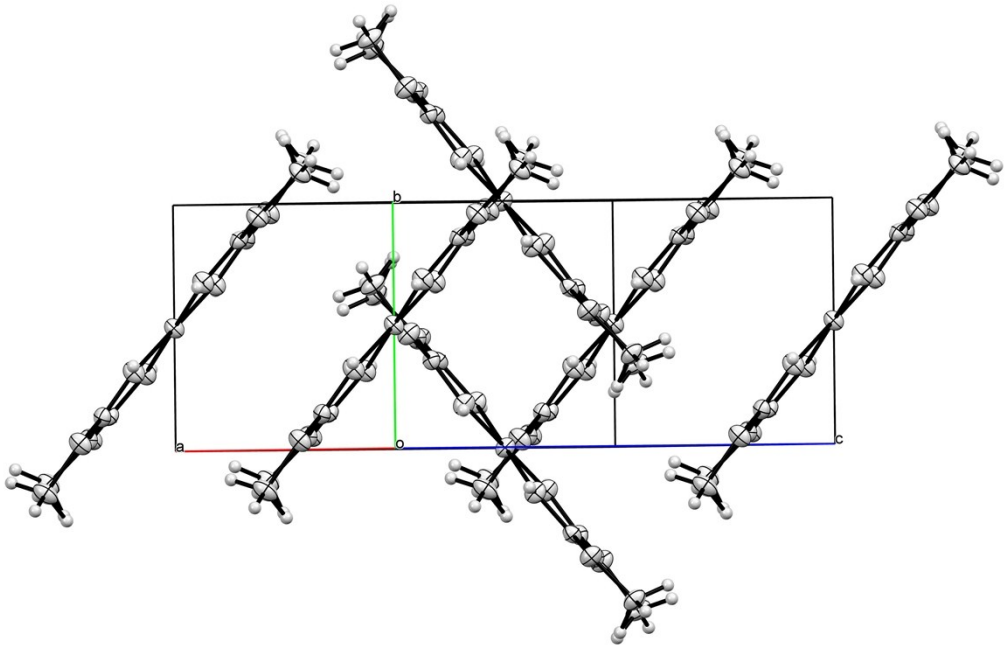

Figure S2. Projection of the structure of **1** along the [201] direction. Thermal ellipsoids are given at the 50% probability level.

The Ni–N bond lengths [1.8652(16) and 1.8659(16) Å] and the N2–Ni1–N3 bond angle [89.66(8)°] exhibit values characteristic for other 1,3,5-triazapentadienate nickel(II) species.[10] The N3–C2 [1.306(2) Å] and N2–C3 [1.302(2) Å] bond distances are shorter than N1–C2 [1.330(2) Å] and N1–C3 [1.337(2) Å] in accordance with their double- and single-bond characters, respectively.[10a] Bond lengths and angles in the structure agree well with those found for the structures of the relevant $[Co(TAP)_3]$ and $[Cu(TAP)_2]$ species.[11] The difference between bond lengths of the TAP ligand is not more than 0.040 Å (for N2–C3 compared with C=N bonds of $[Co(TAP)_3]$) and the largest difference found between bond angles is 1.89° for C3–O1–C1 compared to $[Co(TAP)_3]$. The TAP ligands exhibit *anti–anti* conformation as it was found for $[Co(TAP)_3]$ and $[Cu(TAP)_2]$.[11] It is known for the relevant copper complexes $[Cu(TAP)_2]$, $[Cu(TAP\text{-}H)(TAP)]^+$, and $[Cu(TAP\text{-}H)_2]^{2+}$ that the protonation of the TAP ligand leads to conformational change. The *anti–anti* conformation observed for the anionic ligand $\{HN{=}C(OMe)NC(OMe){=}NH\}^-$ was changed to *syn–syn* for the neutral ligand

HN=C(OMe)NHC(OMe)=NH and its protonation is accompanied by significant changes of geometrical parameters.[12]

Characterization of complexes 2–4

Complexes **2**–**4** were characterized by C, H, and N elemental analyses, high resolution ESI-MS, FTIR, ^{1}H and ^{13}C{^{1}H} NMR spectroscopies, TG-DTA, and also by XRD. Complexes **2**–**4** give satisfactory C, H, and N elemental analyses for the proposed formulas. The positive mode HRESI-MS of these complexes exhibit several groups of peaks corresponding to $[M + H]^+$ (**2**–**4**), $[M – Ni – TAP + 2H]^+$ (**3**), $[M – Ni – 2R'_2Pz + H]^+$ (**2**, **3**), $[M + Ni + 2R'_2Pz + H]^+$ (**2**), and $[TAP + 2H]^+$ (**3**). In the IR spectra of **2**–**4**, the TAP species exhibit weak narrow double bands at 3376–3340 cm^{-1}, which, similarly to those in **1**, can be attributed to ν(N−H). The spectra also display two strong absorption bands at 1618–1614 and 1232–1222 cm^{-1} assigned to ν(C=N) and ν(C–N) of the TAP ligand and these stretches were also found in **1**. The MeO groups exhibit strong bands in the narrow range 1400–1394 cm^{-1} from the ν(C–O). The spectra of **2**–**4** also display strong absorption bands at 1526–1522 cm^{-1} assigned to ν(C=N) of the the azoles cycles.

In the ^{1}H and ^{13}C{^{1}H} NMR spectra of **2**–**4**, the signal of the OMe group appears in the interval 3.6–3.8 ppm, and at *ca*. 54 ppm, correspondingly. The characteristic feature of the ^{13}C{^{1}H} NMR spectra of **2**–**4** is the presence of the signal in the range 161–164 ppm from the C=N carbon of the TAP ligand. The signals from the azolate moiety were also observed (in ^{1}H NMR, $CH_{pyrazolate}$ appears at 5.38 for **2** and **4** and at 6.37 ppm for **3**; in ^{13}C{^{1}H} NMR, $CH_{pyrazolate}$ appears at 147–148 ppm for **2** and **4** and at 153 ppm for **3**).

Thermal properties of 2–4. Compounds **2**–**4** are rather thermally stable and their decomposition starts only at 245, 295, and 280 °C, respectively. In all three cases, the DTA curves exhibit endothermic effects between 300 and 350 °C. The weight loss corresponding to approximately two (for **2** observed –32.9%, calc. –33.8%; **Figure S29**) and four (for **4** observed –41.9%, calc. –47.1%; **Figure S30**) HMe_2Pz. The final product of decomposition of complexes **2** and **4** is the metallic nickel. Weight-loss (TG) is 19.3 and 22.7% for **2** and **4**, respectively, and it is approximately corresponds to the calculated value for metallic Ni (20.7 and 21.6%). The

decomposition of **3** proceeds in two poorly resolved steps and continues even after 1010 °C (**Figure S31**).

X-ray crystallographic studies for 2–5

Dinuclear complexes **2** and **3** display a saddle-shaped structure, where the Ni–N_{imine} [1.838(2)–1.857(2) Å] and Ni–$N_{pyrazole}$ [1.875(3)–1.9142(19) Å] bond distances exhibit values characteristic for [Ni(HN=C(R)NC(R)=NH)$_2$] (R = 3-py, 4-py, 3-(Cl)-4-py, 4-(NC)C_6H_4, CCl_3, NH_2, N(H or Me)$_2$) [1.8472(16)–1.869(2) Å][10a, 13] and the dinuclear {Ni(μ_2-Me_xPz)$_2$Ni} species (x = 2, 3) [1.874(3)–1.917(3) Å].[14] The difference between bond lengths of the [HN=C(OMe)NC(OMe)=NH]$^-$ ligands in the structures of dimers **2** and **3**, and also in **1** is not more than 0.01 Å (for C2–O2 in the structure of **3**) and the largest difference between bond angles is 2.34° for the N8–C10–O3 angle in the structure of **3**. In the structures of **2** and **3**, the molecules form parquet laying (**Figure S3**) and crossed stacks (**Figure S4**), correspondingly.

Trinuclear complexes **4** and **5** exhibit double boat conformation about the central Ni(2) atom. The Ni–N_{imine} and the Ni–N_{azole} bond lengths also are consistent with these values for [Ni(HN=C(R)NC(R)=NH)$_2$] (see before)[10a] and the trinuclear {Ni(μ_2-Me_2Pz)$_2$Ni(μ_2-Me_2Pz)$_2$Ni} species [1.865(2)–1.910(2) Å][14a, 15] ([1.840(3)–1.850(3) Å] and [1.878(3)–1.890(2) Å], respectively). The differences between geometric characteristics of TAP ligands in the structures of **4** and **5**, and also in **1** somewhat higher than in the case of dinuclear species **2** and **3**. The largest difference between bond lengths is 0.038 Å for O2–C4A in the structure of **5** and the largest difference between bond angles is 6.5° for the C3–O1–O1A angle in the same structure. In the structures of **4** and **5**, the molecules form stacks (**Figures S5** and **S6**, respectively).

Complex **5** crystallizes in one of six possible regioisomeric forms, in which all indazolate ligands coordinates to the central Ni atom thought their N1 and to peripheral Ni's thought the N2 centers. In the structure of **5**, the OMe groups of the TAP ligands are disordered in two positions with the occupancies 0.75 for C1, 0.25 for C1A, and 0.5 for C4 and C4A. Disorder of the methoxy groups is due to *syn*- and *anti*-conformations of the TAP ligands; complexes **2**–**4** adopt the *anti–anti* conformations.

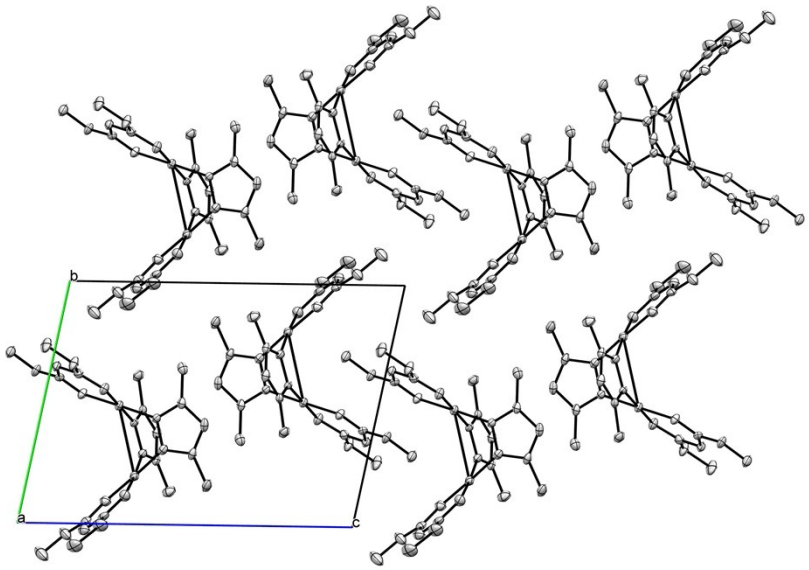

Figure S3. Projection of the structure of **2** on the [011] direction. Thermal ellipsoids are given at the 50% probability level.

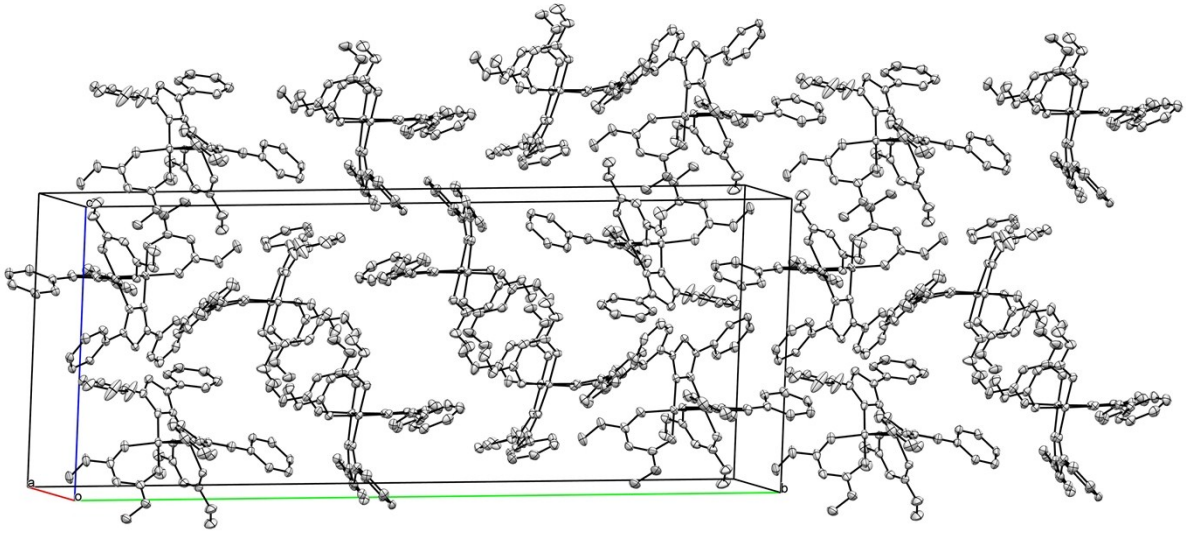

Figure S4. Projection of the structure of **3** on the [110] direction. Thermal ellipsoids are given at the 50% probability level.

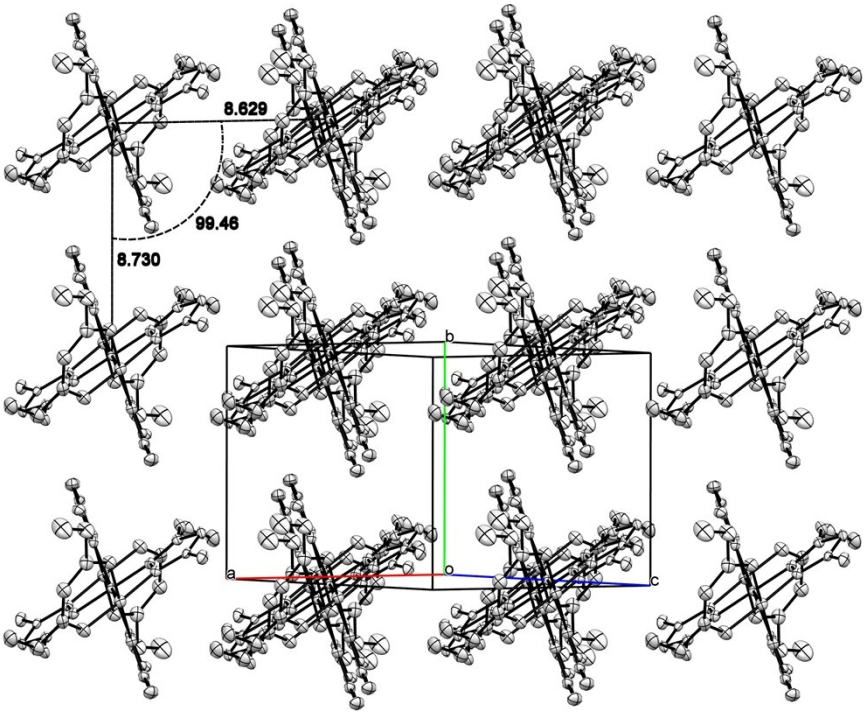

Figure S5. Projection of the structure of **4** on the [101] direction. Thermal ellipsoids are given at the 50% probability level.

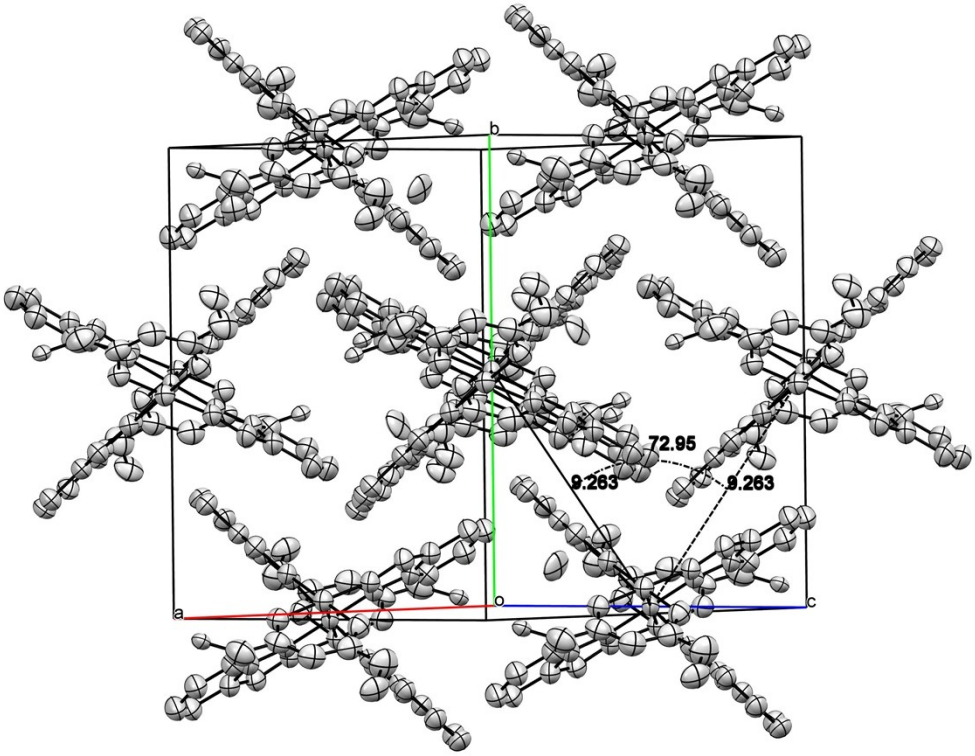

Figure S6. Projection of the structure of **5** on the [101] direction. Thermal ellipsoids are given at the 50% probability level.

Results of theoretical calculations

Theoretical verification of the existence of metallophilic interactions Ni•••Ni in dimeric and trimeric clusters. Inspection of the crystallographic data suggests the presence of metallophilic interactions Ni•••Ni in dimeric and trimeric structures **2**–**4**. Indeed, results of the X-ray analysis reveals that the interatomic distances between the Ni atoms in ([$Ni_2(\mu_2$-$Me_2Pz)_2L_2$]) {**2**, 3.099 Å}, ([$Ni_2(\mu_2$-$Ph_2Pz)_2L_2$]) {**3**, 2.986}, and ([$Ni_3(\mu_2$-$Me_2Pz)_4L_2$]) {**4**, 3.245 Å} clusters are less than sum of their Bondi's (the shortest) van der Waals radii (1.63 Å for Ni atom).[17] We carried out theoretical DFT calculations and performed topological analysis of the electron density distribution within the formalism of Bader's theory (AIM method)[18] in order to confirm or refute this assumption and quantitatively estimate the energies of these non-covalent interactions. The results of this theoretical study are summarized in **Table S1**, the contour line diagrams of the Laplacian distribution $\nabla^2\rho(\mathbf{r})$, bond paths, and selected zero-flux surfaces for **2**, **3**, and **4** are shown in **Figures S7**.

Table S1. Values of the density of all electrons – $\rho(\mathbf{r})$, Laplacian of electron density – $\nabla^2\rho(\mathbf{r})$, energy density – H_b, potential energy density – $V(\mathbf{r})$, and Lagrangian kinetic energy – $G(\mathbf{r})$ (Hartree) at the bond critical points (3, –1), corresponding to metallophilic interactions Ni•••Ni in **3**, as well as energies for these interactions E_{int} (kcal/mol), defined by two approaches.

Method/basis	$\rho(\mathbf{r})$	$\nabla^2\rho(\mathbf{r})$	H_b	V(r)	G(r)	E_{int}[a]	E_{int}[b]
M06/6-311+G*	0.017	0.052	-0.001	-0.014	0.014	4.39	3.77
M06/DZP-DKH	0.016	0.046	-0.001	-0.014	0.013	4.39	3.50

[a] $E_{int} = -V(\mathbf{r})/2$ [19]

[b] $E_{int} = 0.429G(\mathbf{r})$ [20]

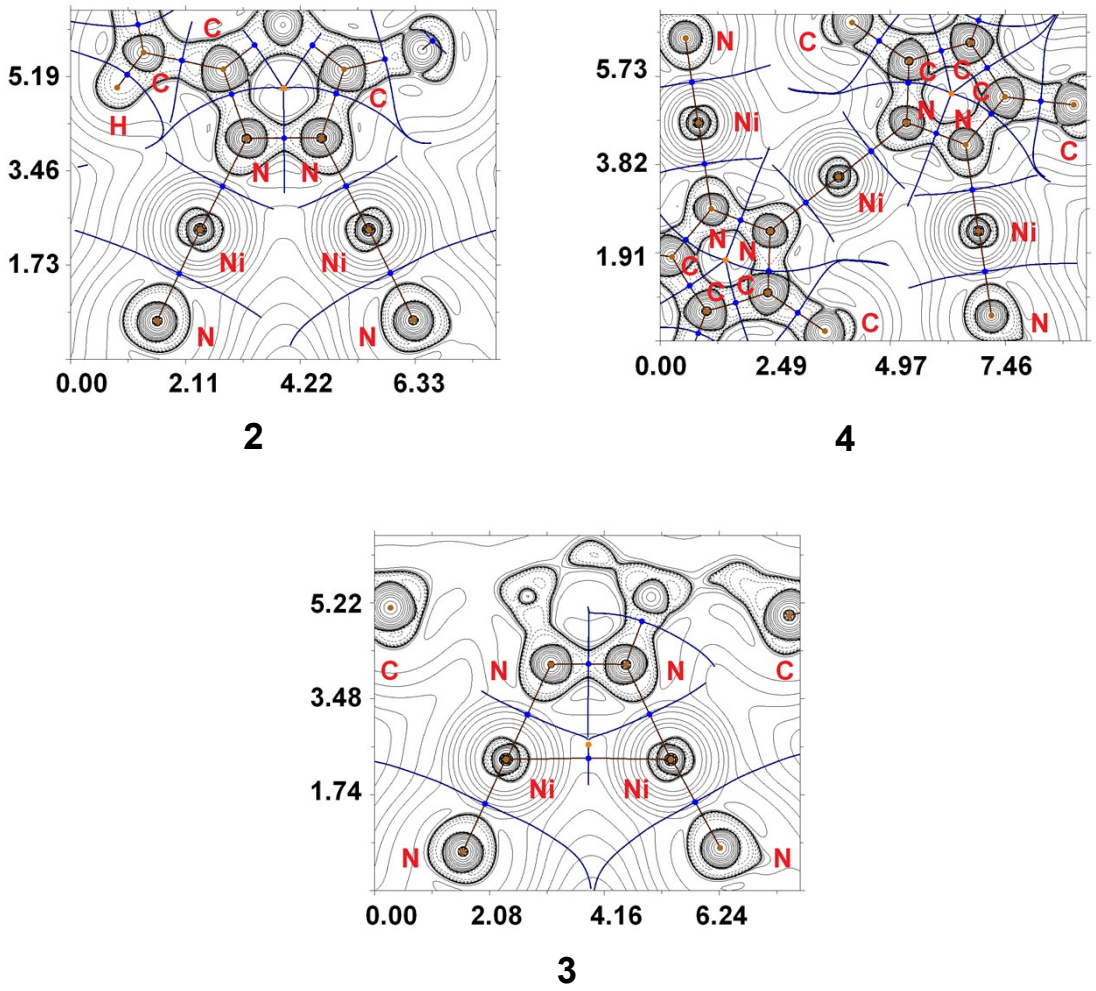

Figure S7. Contour line diagrams of the Laplacian distribution $\nabla^2\rho(\mathbf{r})$, bond paths and selected zero-flux surfaces for **2**, **3**, and **4**. Bond critical points (3, –1) are shown in blue, nuclear critical points (3, –3) – in pale brown, ring critical points (3, +1) – in orange, length unit – Å.

The AIM analysis did not reveal any metallophilic interactions Ni•••Ni in **2** and **4** clusters, appropriate bond critical points (BCPs) (3, –1) for these contacts were not located (**Figure S7**). However, for **3** with the shortest Ni•••Ni distance we succeeded to find appropriate BCP. The balance between the Lagrangian kinetic energy G(**r**) and potential energy density V(**r**) at the BCPs reveals the nature of these interactions, if the ratio $-G(\mathbf{r})/V(\mathbf{r}) > 1$ is satisfied, than the nature of appropriate interaction is purely noncovalent, in case the $-G(\mathbf{r})/V(\mathbf{r}) < 1$ some covalent component

takes place.[21] Based on this criterion we can state that the covalent contribution in the metallophilic interactions Ni•••Ni in **3** is negligible.

Table S2. Cartesian atomic coordinates for the clusters **2**–**4**.

Atom	X	Y	Z
2			
Ni	6.199226	5.824058	3.183784
Ni	6.233689	3.005424	4.470289
O	7.406031	6.532736	-0.609086
N	7.042290	5.985395	1.542541
H	7.857300	5.713846	1.504438
N	7.808215	5.242506	3.978886
N	5.377061	4.369885	5.429754
N	5.366422	5.629923	4.871285
N	5.303256	6.904537	0.211465
N	7.823061	4.021690	4.600205
N	7.091780	1.696729	3.479610
H	7.948039	1.758296	3.427868
N	4.614455	6.381420	2.419895
H	3.922458	6.365067	2.930138
O	7.414126	-0.039991	2.103682
O	3.138444	7.165241	0.912505
N	4.632863	2.101062	4.246310
H	3.954179	2.427707	4.660945
N	5.277937	0.301936	2.849995
O	3.094475	0.639069	3.499434
C	6.538560	6.465009	0.437271
C	4.576921	5.781985	6.934473
H	4.218626	6.128481	7.719031

C	9.763764	5.034079	5.005419
H	10.620443	5.211262	5.320366
C	9.253764	7.240852	3.717508
H	9.582695	7.195222	2.817657
H	9.911485	7.659666	4.278508
H	8.442859	7.754488	3.737192
C	4.898113	4.473459	6.694045
C	4.887384	6.495640	5.781540
C	9.312520	2.676797	6.047277
H	8.578330	2.497930	6.639210
H	10.108799	2.831916	6.561879
H	9.447034	1.922639	5.467998
C	4.840345	3.268242	7.591083
H	4.778411	2.473400	7.056797
H	4.071528	3.331204	8.163332
H	5.635833	3.230842	8.128181
C	4.411390	1.031408	3.537537
C	4.766527	7.952364	5.508773
H	5.401787	8.205831	4.835291
H	4.943134	8.445114	6.314420
H	3.879062	8.148796	5.202261
C	4.417041	6.799736	1.195114
C	6.545555	0.692138	2.851401
C	9.007776	3.884682	5.226163
C	8.978891	5.855215	4.220862
C	6.906257	7.087741	-1.839070
H	7.576101	7.007572	-2.522394

H	6.691430	8.013797	-1.708310
H	6.116605	6.610568	-2.107619
C	2.879311	7.686839	-0.409151
H	3.210431	7.070364	-1.067167
H	3.321970	8.531702	-0.511790
H	1.934028	7.803831	-0.527256
C	2.777931	-0.450402	2.603943
H	2.990535	-0.196463	1.702686
H	1.841656	-0.655077	2.665807
H	3.290608	-1.224396	2.847183
C	6.857316	-1.089225	1.286505
H	6.250670	-0.709191	0.646768
H	6.385460	-1.712811	1.843288
H	7.564959	-1.545314	0.823926
3			
Ni	4.831949	22.905742	11.836248
Ni	2.048760	21.872208	12.152363
O	6.896515	23.445373	8.432114
O	5.358245	26.835141	11.100206
O	-0.204422	21.111473	8.884976
O	-0.919506	24.597015	11.765372
N	6.153764	25.115136	9.810396
N	5.629824	22.828338	10.182696
N	4.835216	24.753237	11.732275
N	4.669079	21.009419	11.895499
N	3.391693	20.529764	12.014971
N	4.143065	22.949625	13.607657

N	2.899678	22.423654	13.765715
N	-0.507960	22.864450	10.317344
N	1.251209	21.293993	10.592936
N	0.832870	23.272666	12.238254
C	7.547738	24.483578	7.681864
C	5.458903	25.509615	10.861747
C	6.190224	23.811591	9.524149
C	6.095077	27.708097	10.224511
C	6.976238	20.083474	11.751165
C	5.512622	19.957869	11.757623
C	4.766245	18.784638	11.777481
C	3.447172	19.177547	11.955397
C	2.282408	18.291638	12.144775
C	0.196760	21.788563	9.984760
C	-1.439820	21.536175	8.259687
C	-0.162569	23.522699	11.420357
C	-2.058056	24.891795	10.930524
C	6.166796	23.359020	15.030176
C	4.743120	23.021063	14.822716
C	3.849520	22.544941	15.780265
C	2.709133	22.157136	15.081678
C	1.533749	21.419991	15.600896
C	1.748746	20.491298	16.631258
C	0.704530	19.734134	17.123513
C	-0.577522	19.888786	16.609139
C	-0.797330	20.807273	15.593630
C	0.250874	21.571502	15.091527

C	1.148702	18.694360	12.857246
C	0.086911	17.813554	13.046463
C	0.148951	16.520213	12.547265
C	1.276320	16.097474	11.866116
C	2.327125	16.992410	11.642994
C	7.755038	19.026428	11.268273
C	9.143835	19.093156	11.328170
C	9.775223	20.209864	11.863210
C	9.005503	21.257882	12.341258
C	7.620337	21.193901	12.295245
C	6.819605	22.759255	16.110910
C	8.177615	22.927252	16.321923
C	8.930946	23.684415	15.447358
C	8.302694	24.303806	14.368401
C	6.930592	24.157397	14.171111
H	5.636370	22.059007	9.797804
H	4.371192	25.166163	12.327212
H	1.616492	20.613370	10.215470
H	0.933862	23.822974	12.891473
H	8.058447	24.091062	6.972945
H	6.886150	25.069997	7.308757
H	8.128038	24.983643	8.261302
H	5.779490	27.601725	9.323630
H	5.975093	28.619127	10.500587
H	7.029154	27.487895	10.264873
H	5.086016	17.915608	11.689491
H	-1.663698	20.932878	7.549315

H	-2.144730	21.537353	8.911938
H	-1.330483	22.420514	7.904501
H	-1.758661	25.085698	10.038846
H	-2.646967	24.135809	10.913895
H	-2.524403	25.650921	11.283611
H	3.987083	22.495877	16.698743
H	2.601534	20.384926	16.985798
H	0.859041	19.117492	17.802403
H	-1.282072	19.380870	16.942853
H	-1.653494	20.912860	15.245225
H	0.091682	22.186182	14.412314
H	1.103009	19.555147	13.206781
H	-0.669795	18.093810	13.510142
H	-0.565890	15.938505	12.670289
H	1.335247	15.221770	11.558396
H	3.066995	16.716471	11.152192
H	7.342581	18.275545	10.905661
H	9.653303	18.384664	11.007857
H	10.702997	20.253041	11.898728
H	9.421575	22.010335	12.696282
H	7.116628	21.899645	12.630896
H	6.330579	22.234461	16.702456
H	8.585625	22.528063	17.056674
H	9.846885	23.780189	15.576356
H	8.802449	24.818394	13.776370
H	6.518464	24.595053	13.461385
4			

Ni	-0.973585	-2.075568	5.900634
Ni	0.703818	-2.425224	8.656466
N	0.905575	-4.106291	9.402070
O	0.955207	-5.774122	10.890210
N	0.683406	-2.978455	5.897093
O	-0.990416	-1.863929	12.273200
N	1.458010	-3.020063	7.028835
N	-0.129703	-0.593235	6.690139
N	0.083354	-3.776161	11.601826
N	0.514939	-0.712691	7.893868
N	-0.109405	-1.868422	10.219898
C	-0.307162	-2.539526	11.315055
C	-0.040041	0.678945	6.290076
C	0.640165	-4.486022	10.621141
C	2.631237	-3.575963	6.726723
C	0.650468	1.404028	7.249519
H	0.853771	2.310881	7.227096
C	-0.623184	1.139460	4.993116
H	-0.413444	0.504033	4.305102
H	-0.254495	1.995378	4.762992
H	-1.576588	1.215070	5.079266
C	2.635417	-3.911255	5.383738
H	3.325621	-4.313137	4.908147
C	0.978771	0.495786	8.252626
C	1.393867	-3.522437	4.892806
C	3.744475	-3.720967	7.721569
H	3.589770	-4.497898	8.263248

H	3.776739	-2.941268	8.280949
H	4.578704	-3.815736	7.256599
C	1.800429	0.708662	9.485859
H	1.549639	0.065972	10.152631
H	1.648179	1.595233	9.822195
H	2.730258	0.603832	9.272256
C	0.858192	-3.624194	3.497896
H	0.494827	-2.775628	3.232367
H	0.168583	-4.291070	3.467212
H	1.566956	-3.869242	2.899571
C	-1.349618	-2.593161	13.469967
H	-1.950797	-2.063130	13.999844
H	-0.558460	-2.783269	13.978601
H	-1.779331	-3.416085	13.226861
C	0.716240	-6.257424	12.222573
H	1.323512	-5.830980	12.831518
H	0.852644	-7.207300	12.247356
H	-0.187201	-6.057320	12.478660
H	-0.462239	-1.114362	10.267103
H	1.207875	-4.764772	8.992566
Ni	-2.650988	-1.725913	3.144802
N	-2.852746	-0.044845	2.399198
O	-2.902377	1.622986	0.911058
N	-2.630576	-1.172681	5.904174
O	-0.956755	-2.287208	-0.471933
N	-3.405181	-1.131074	4.772433
N	-1.817467	-3.557901	5.111129

N	-2.030524	-0.374976	0.199441
N	-2.462110	-3.438446	3.907400
N	-1.837766	-2.282714	1.581370
C	-1.640009	-1.611611	0.486212
C	-1.907130	-4.830081	5.511192
C	-2.587336	0.334885	1.180127
C	-4.578407	-0.575174	5.074545
C	-2.597638	-5.555165	4.551749
H	-2.800941	-6.462017	4.574171
C	-1.323986	-5.290597	6.808151
H	-1.533727	-4.655169	7.496165
H	-1.692675	-6.146514	7.038276
H	-0.370582	-5.366206	6.722002
C	-4.582588	-0.239882	6.417529
H	-5.272791	0.162000	6.893120
C	-2.925941	-4.646923	3.548641
C	-3.341038	-0.628700	6.908462
C	-5.691646	-0.430170	4.079698
H	-5.536940	0.346762	3.538020
H	-5.723909	-1.209868	3.520318
H	-6.525874	-0.335401	4.544668
C	-3.747599	-4.859799	2.315409
H	-3.496810	-4.217108	1.648637
H	-3.595350	-5.746369	1.979073
H	-4.677429	-4.754969	2.529012
C	-2.805362	-0.526942	8.303372
H	-2.441998	-1.375508	8.568900

H	-2.115753	0.139933	8.334055
H	-3.514126	-0.281894	8.901696
C	-0.597553	-1.557975	-1.668699
H	0.003626	-2.088006	-2.198576
H	-1.388710	-1.367867	-2.177334
H	-0.167839	-0.735051	-1.425593
C	-2.663410	2.106287	-0.421305
H	-3.270683	1.679844	-1.030251
H	-2.799815	3.056163	-0.446088
H	-1.759970	1.906184	-0.677393
H	-1.484932	-3.036775	1.534165
H	-3.155046	0.613635	2.808702

Table S3. Crystal data and structure refinement for **1**–**5**.

Identification code	**1**	**2**	**3**	**4**	**5**
Empirical formula	$C_8H_{16}N_6NiO_4$	$C_{18}H_{30}N_{10}Ni_2O_4$	$C_{76}H_{76}N_{20}Ni_4O_8$	$C_{14}H_{22}N_7Ni_{1.5}O_2$	$C_{36}H_{36}N_{14}O_4Ni_3$
Formula weight	318.98	567.94	1632.40	408.45	904.92
Temperature/K	100(2)				100.00(10)
Crystal system	monoclinic	triclinic	monoclinic	triclinic	monoclinic
Space group	$P2_1/n$	P-1	$P2_1/n$	P-1	$P2_1/c$
a/Å	9.8999(5)	8.1705(4)	11.83295(18)	8.6286(4)	13.6333(12)
b/Å	5.7496(3)	10.6165(7)	39.2516(5)	8.7296(4)	14.8982(4)
c/Å	11.1292(5)	14.8093(8)	16.3620(3)	12.6607(5)	11.0132(5)
α/°	90	78.021(5)	90	107.345(4)	90
β/°	98.159(4)	75.628(5)	99.3458(14)	98.847(4)	112.089(6)
γ/°	90	86.402(5)	90	99.464(4)	90
Volume/Å^3	627.06(5)	1217.20(12)	7498.68(19)	876.83(6)	2072.7(2)
Z	2		4	2	
ρ_{calc}mg/mm^3	1.689	1.550	1.446	1.547	1.450

m/mm^{-1}	2.470	1.592	1.697	1.650	2.044
F(000)	332.0	592.0	3392.0	426.0	932.0
Crystal size/mm^3	0.26 × 0.18 × 0.10	0.32 × 0.18 × 0.12	0.25 × 0.2 × 0.11	0.34 × 0.28 × 0.22	0.21 × 0.19 × 0.16
2Θ range for data collection	12.92 to 151.74°	5.14 to 53°	7.09 to 144.99	5.02 to 54.98°	7 to 139.98°
Index ranges	-8 ≤ h ≤ 12, -7 ≤ k ≤ 7, -13 ≤ l ≤ 9	-10 ≤ h ≤ 10, -13 ≤ k ≤ 13, -18 ≤ l ≤ 16	-14 ≤ h ≤ 10, 0 ≤ k ≤ 48, -10 ≤ l ≤ 20	-10 ≤ h ≤ 10, -11 ≤ k ≤ 11, -16 ≤ l ≤ 16	-16 ≤ h ≤ 15, -18 ≤ k ≤ 16, -13 ≤ l ≤ 12
Reflections collected	2615	10684	14876	9527	9619
Independent reflections	1263[R(int) = 0.0212]	4942[R(int) = 0.0377]	14876 [Rint = N/A, Rsigma = 0.0390]	3888[R(int) = 0.0376]	3845[R(int) = 0.0228]
Data/restraints/parameters	1263/0/98	4942/0/315	14876/0/981	3888/0/237	3845/2/289
Goodness-of-fit on F^2	1.142	1.046	1.046	1.036	1.052
Final R indexes [I>=2σ (I)]	R_1 = 0.0324, wR_2 = 0.0962	R_1 = 0.0417, wR_2 = 0.0744	R1 = 0.0442, wR2 = 0.1089	R_1 = 0.0439, wR_2 = 0.0845	R_1 = 0.0573, wR_2 = 0.1744
Final R indexes [all data]	R_1 = 0.0360, wR_2 = 0.0991	R_1 = 0.0613, wR_2 = 0.0818	R1 = 0.0579, wR2 = 0.1168	R_1 = 0.0660, wR_2 = 0.0918	R_1 = 0.0648, wR_2 = 0.1855
Largest diff. peak/hole / e Å^{-3}	0.32/-0.41	0.48/-0.35	1.61/-0.42	0.52/-0.38	0.73/-0.33

Table S4. Selected bond lengths (Å) and angles (°) for complexes **2**–**5**.

	2	**3**	**4**	**5**
Ni1–N2	1.845(2)	1.855(2)	1.852(3)	1.840(3)
Ni(A1)–N(A2)		1.838(2)		
Ni1–N3	1.852(2)	1.844(2)	1.849(3)	1.844(3)
Ni(A1)–N(A3)		1.851(2)		
Ni1–N4	1.892(2)	1.901(2)	1.888(2)	1.883(3)
Ni(A1)–N(A4)		1.904(2)		
Ni1–N6	1.887(2)	1.9033(19)	1.885(2)	1.890(3)[1]
Ni(A1)–N(A6)		1.901(2)		
Ni2–N5	1.875(3)	1.9142(19)	1.887(2)	1.878(3)
Ni(A2)–N(A5)		1.904(2)		
Ni2–N7	1.890(2)	1.906(2)	1.881(2)	1.883(3)
Ni(A2)–N(A7)		1.906(2)		
Ni2–N10	1.852(3)	1.849(2)		
Ni(A2)–N(A10)		1.857(2)		
N3–C2	1.306(3)	1.307(3)	1.301(4)	1.327(5)
NA3–CA2		1.311(3)		
N2–C3	1.310(4)	1.307(3)	1.305(4)	1.307(6)
NA2–CA3		1.311(3)		
N9–C10	1.303(4)	1.310(3)		
NA9–CA10		1.313(3)		
N10–C12	1.305(4)	1.313(3)		
NA10–CA12		1.312(3)		
N1–C3	1.328(4)	1.330(4)	1.330(4)	1.312(6)
N(A1)–C(A3)		1.335(4)		
N1–C2	1.331(3)	1.339(4)	1.325(4)	1.331(5)
N(A1)–C(A2)		1.321(4)		
N8–C10	1.324(4)	1.331(4)		
N(A8)–C(A10)		1.329(4)		
N8–C12	1.326(4)	1.330(4)		

N(A8)–C(A12)		1.330(3)		
C3–O1	1.360(3)	1.354(3)	1.353(4)	1.379(5)
C(A3)–O(A1)		1.351(3)		
O1–C1, O1–C(1A)	1.444(3)	1.444(4)	1.437(4)	1.436(6), 1.39(2)
O(A1)–C(A1)		1.437(3)		
C2–O2	1.361(3)	1.348(4)	1.358(4)	1.340(5)
C´2–O´2		1.351(3)		
O2–C4, O2–C(4A)	1.439(3)	1.437(3)	1.445(4)	1.429(7), 1.481(7)
O(A2)–C(A4)		1.440(3)		
C10–O3	1.374(3)	1.359(3)		
C(A10)–O(A3)		1.353(3)		
O3–C11	1.446(4)	1.441(3)		
O(A3)–C(A11)		1.448(4)		
C12–O4	1.360(4)	1.365(3)		
C(A12)–O(A4)		1.359(3)		
O4–C13	1.442(4)	1.450(4)		
O(A4)–C(A13)		1.442(3)		
N2–Ni1–N3	89.87(10)	89.14(10)	88.98(13)	89.16(16)
N(A2)–Ni(A1)–N(A3)		91.71(9)		
N9–Ni2–N10	89.48(12)	88.71(9)		
N(A9)–Ni(A2)–N(A10)		114.96(7)		
Ni1–N2–C3	127.8(2)	128.2(2)	128.1(2)	128.6(3)
Ni(A1)–N(A2)–C(A3)		116.7(2)		
Ni1–N3–C2	127.3(2)	128.9(2)	128.4(2)	129.0(3)
Ni(A1)–N(A3)–C(A2)		117.2(2)		
Ni2–N9–C10	127.9(2)	128.93(19)		
Ni(A2)–N(A9)–C(A10)		114.96(15)		
Ni2–N10–C12	127.4(2)	128.90(19)		
Ni(A2)–N(A10)–C(A12)		134.58(16)		
N4–Ni1–N6	88.16(10)	90.53(9)	88.79(10)	89.94(12)[1]
N(A4)–Ni(A1)–N(A6)		87.88(8)		
N5–Ni2–N7	87.59(10)	90.97(8)	89.10(10)	89.61(12)[1]

N(A5)–Ni(A2)–N(A7)		87.15(8)		
N2–C3–N1		128.2(2)		128.0(4)
N(A2)–C(A3)–N(A1)		127.9(3)		
N3–C2–N1	128.6(3)	127.1(3)	128.2(3)	125.9(4)
N(A3)–C(A2)–N(A1)		127.3(2)		
N9–C10–N8	128.5(3)	127.8(2)		
N(A9)–C(A10)–N(A8)		127.9(2)		
N10–C12–N8	128.8(3)	127.6(2)		
N(A10)–C(A12)–N(A8)		128.3(2)		
C3–N1–C2	117.9(2)	118.2(2)	117.6(3)	119.4(3)
C(A3)–N(A1)–C(A2)		118.5(2)		
C10–N8–C12	117.6(3)	117.7(2)		
C(A10)–N(A8)–C(A12)		118.1(2)		
C3–O1–C1, C3–O1–C(1A)	117.1(2)	116.7(3)	117.8(3)	118.1(4), 123.4(8)
C(A3)–O(A1)–C(A1)		117.6(2)		
C2–O2–C4	117.0(2)	117.7(2)	117.3(3)	122.0(4), 120.3(4)
C(A2)–O(A2)–C(A4)		116.7(2)		
C10–O3–C11	116.2(3)	117.6(2)		
C(A10)–O(A3)–C(A11)		117.2(2)		
C12–O4–C13	117.2(3)	117.1(3)		
C(A12–O(A4)–C(A13)		117.0(2)		

[1]–*X*, 1–*Y*, –*Z*

Spectra of reaction mixtures and complexes 1–5

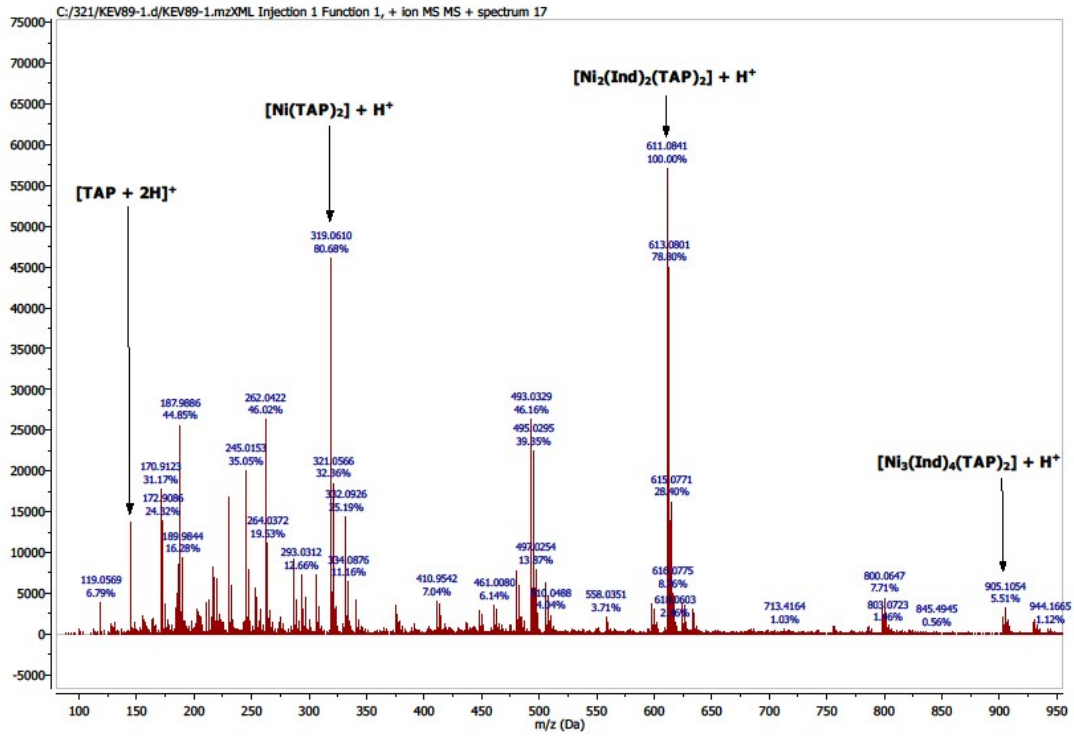

Figure S8. HRESI-MS for the product of reaction $Ni(TAP)_2$ with IndH in MeOH

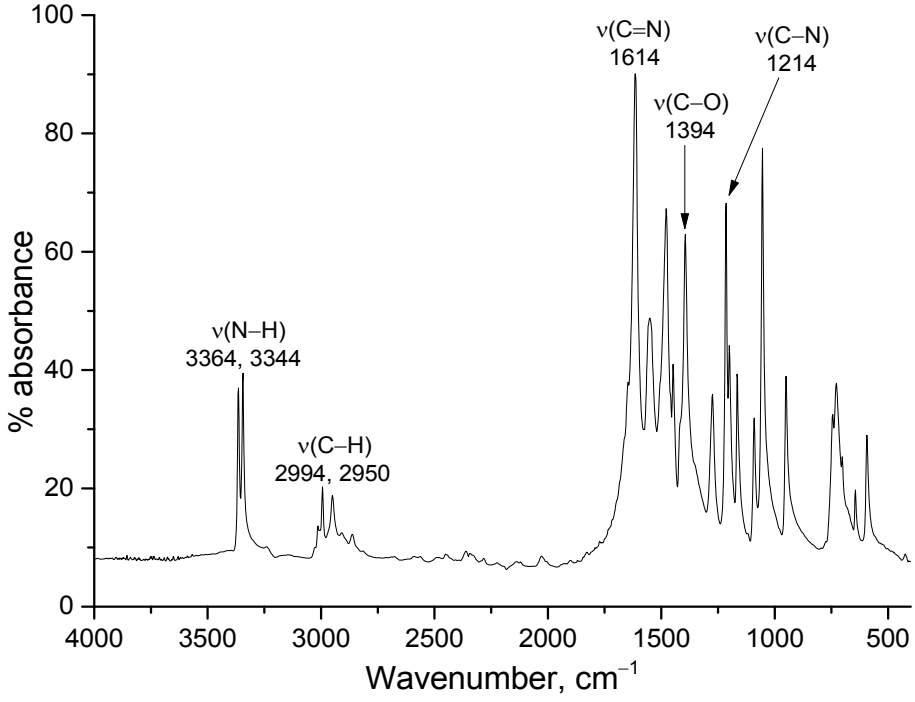

Figure S9. FTIR spectrum of **1**

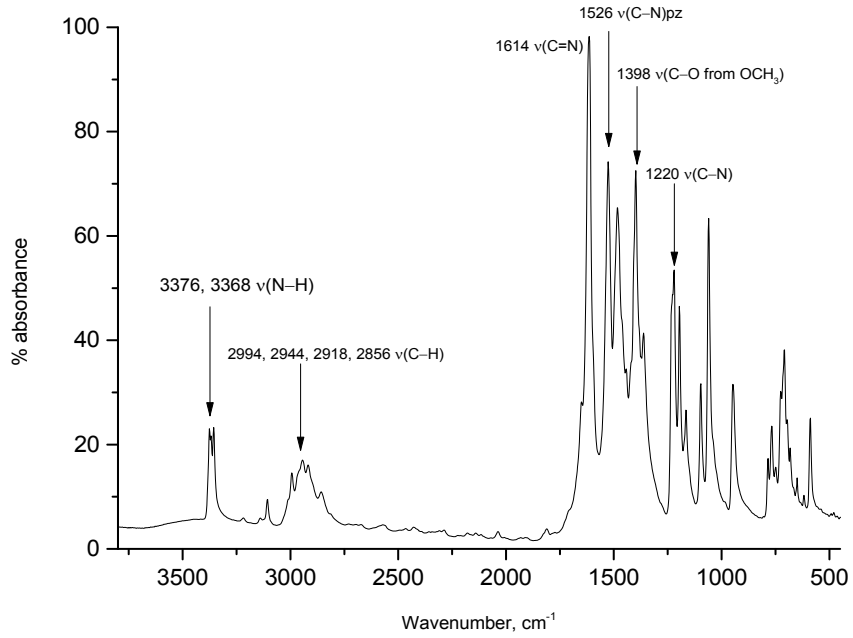

Figure S10. FTIR spectrum of **2**

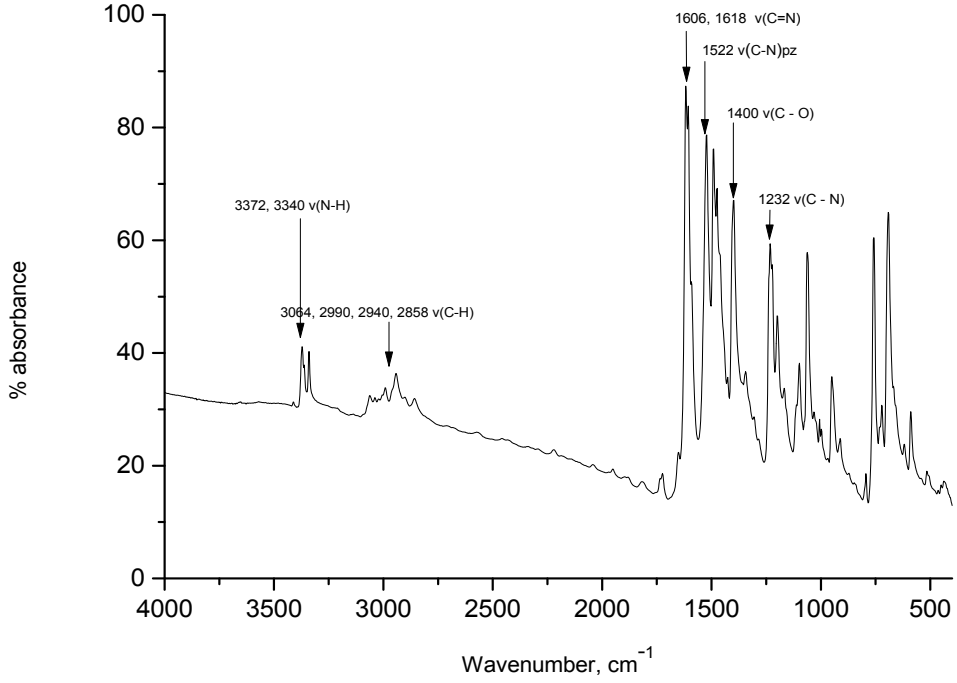

Figure S11. FTIR spectrum of **3**

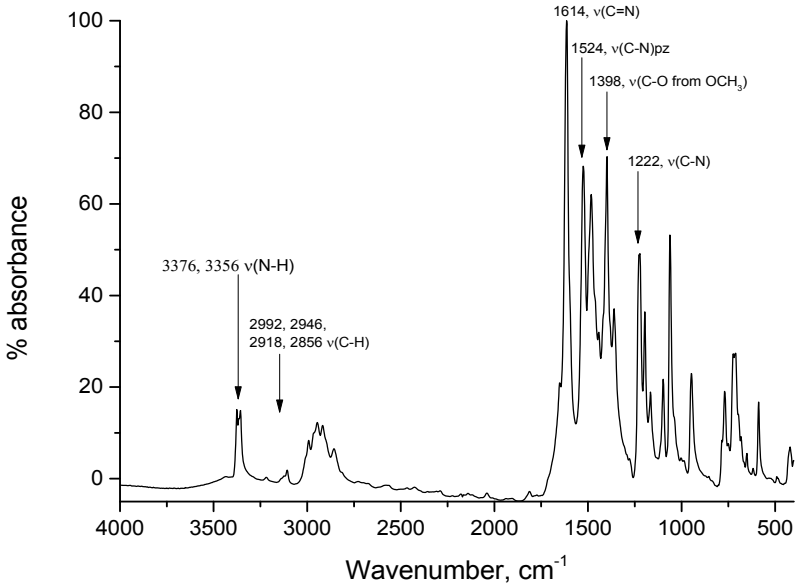

Figure S12. FTIR spectrum of **4**

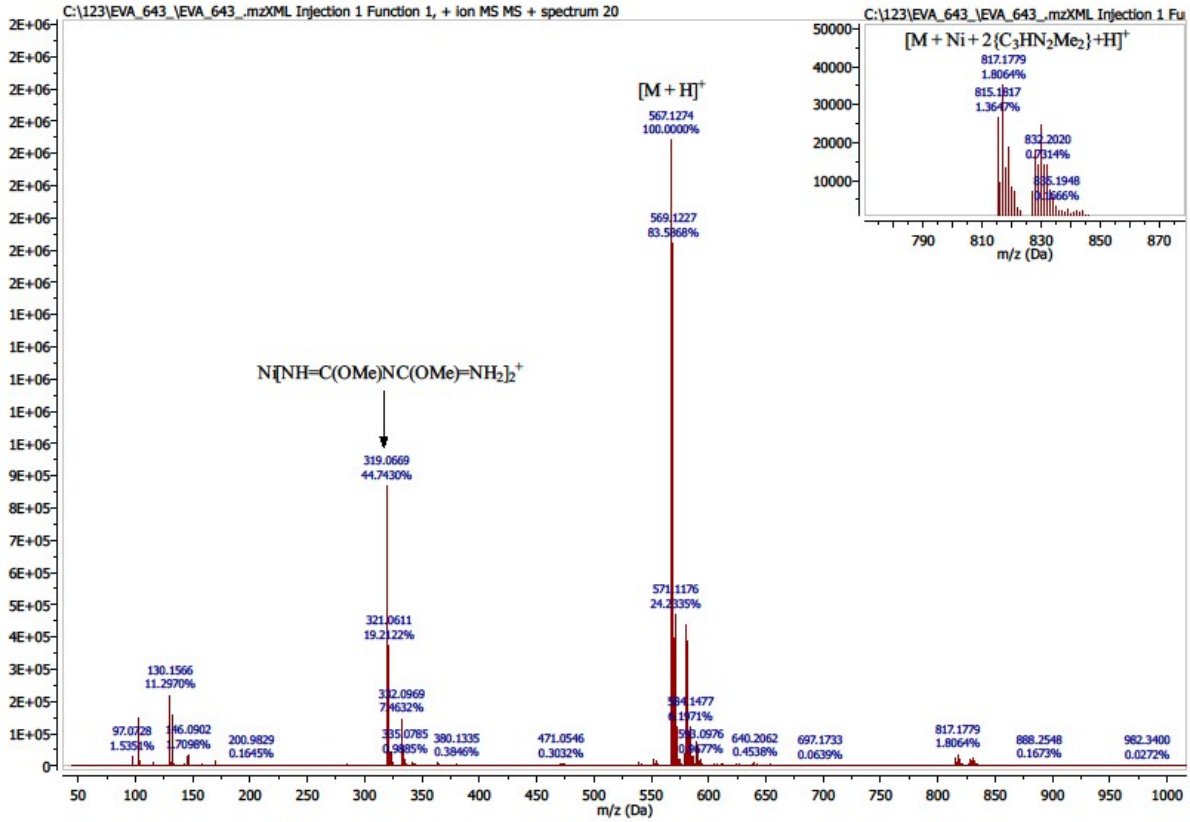

Figure S13. HRESI-MS of **2**

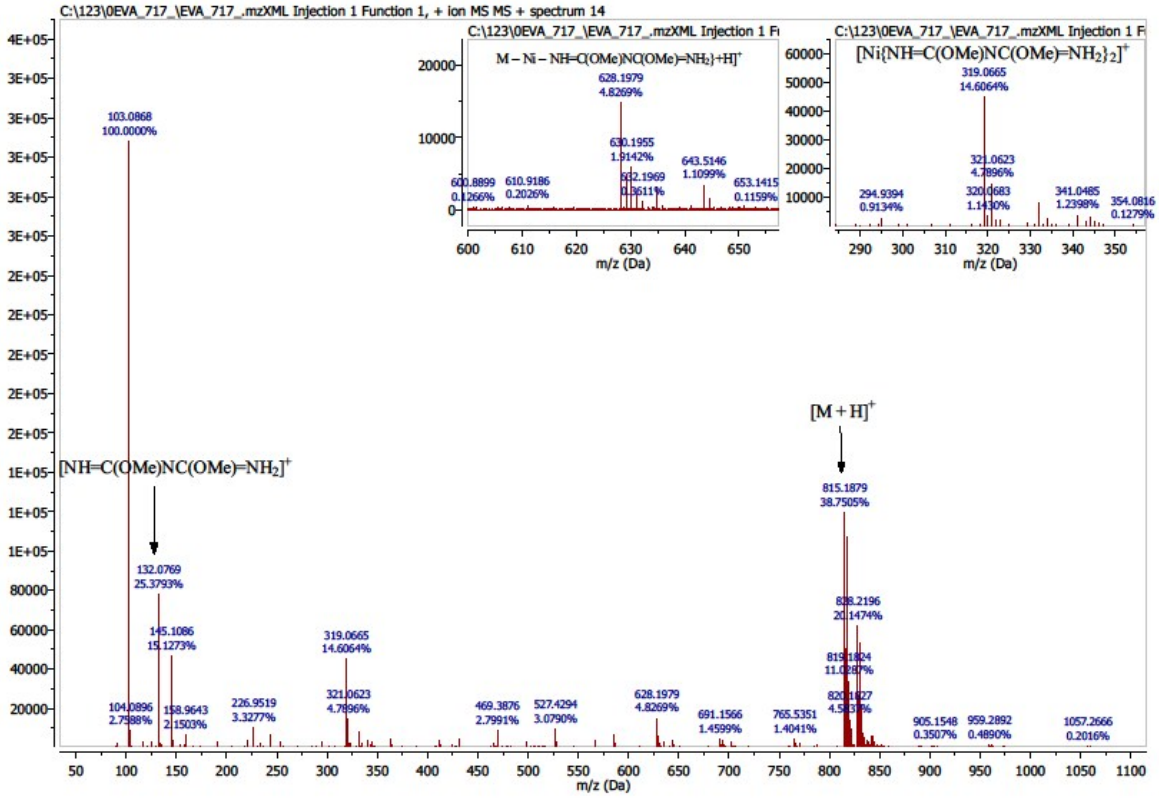

Figure S14. HRESI-MS of **3**

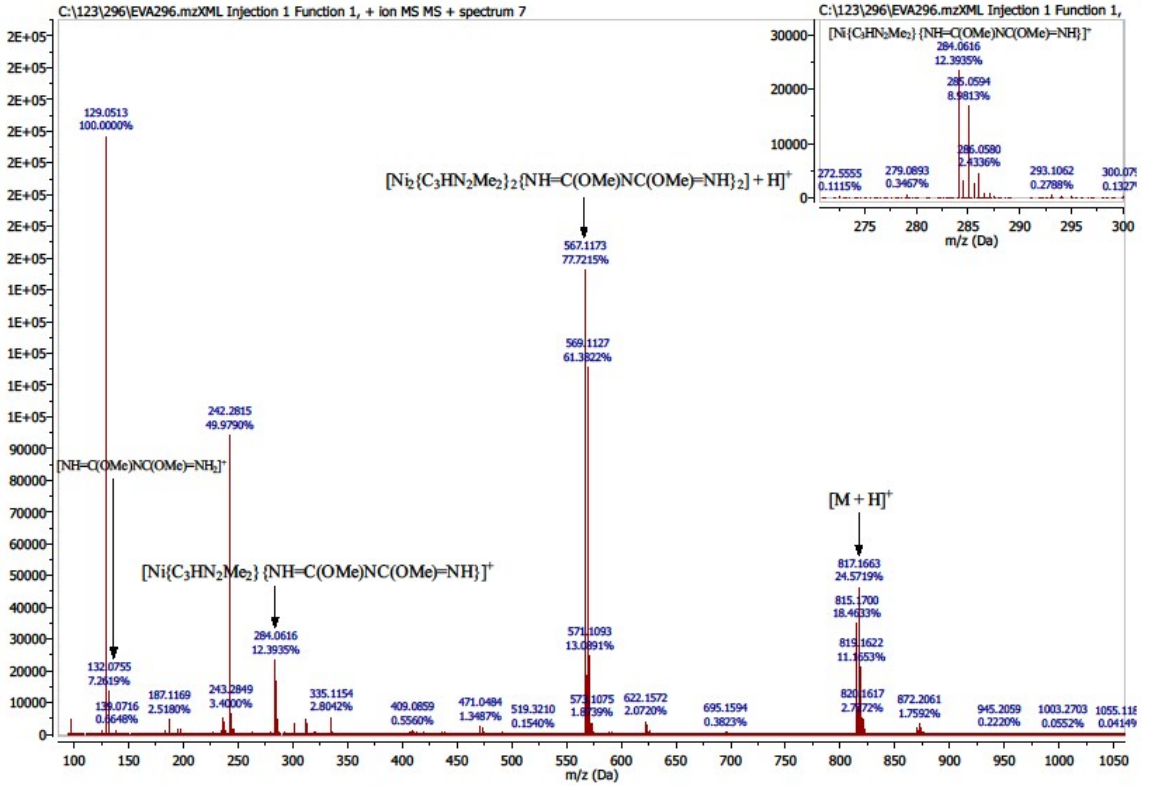

Figure S15. HRESI-MS of **4**

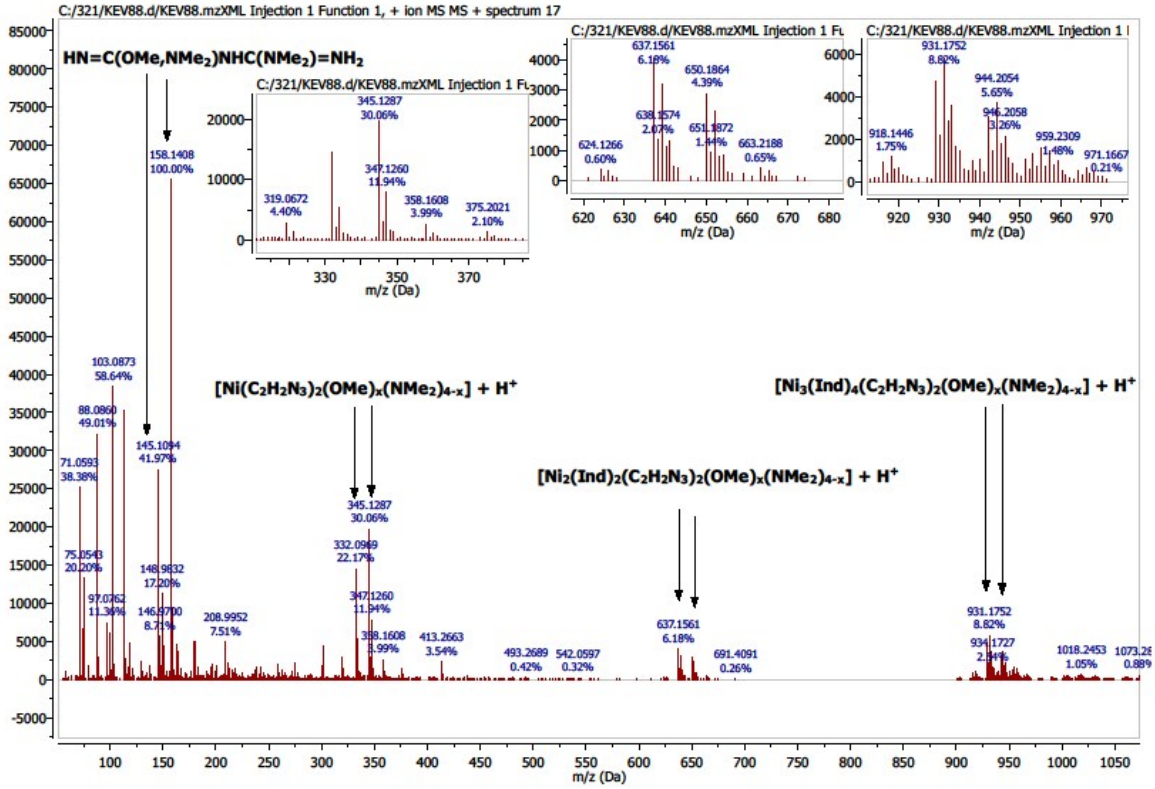

Figure S16. HRESI-MS for the product of reaction $NiCl_2$ with IndH and $NCNMe_2$ in MeOH

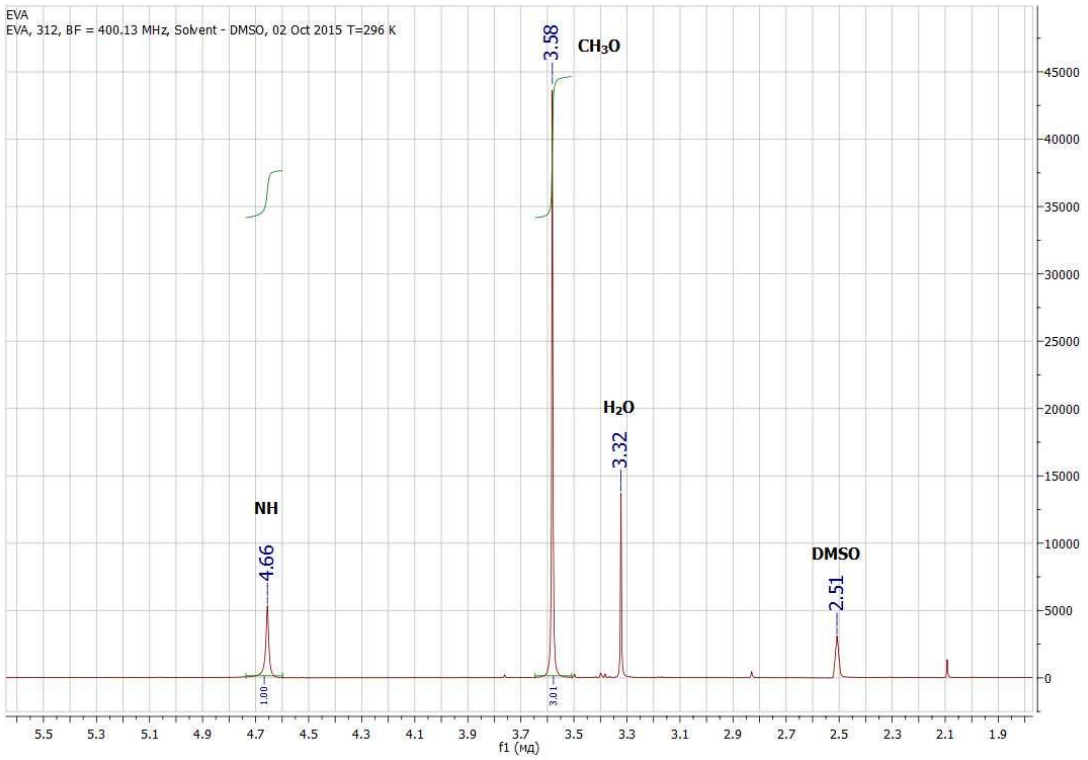

Figure S17. ^{1}H-NMR spectra of **1**

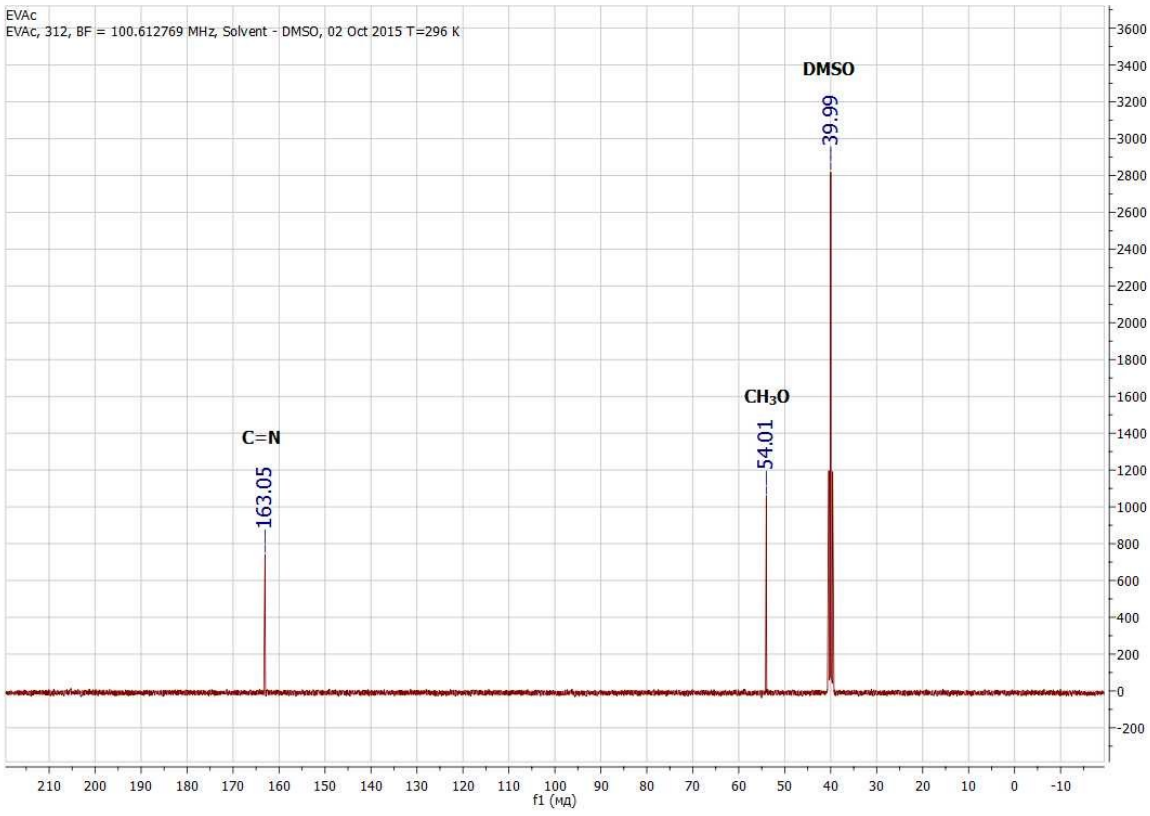

Figure S18. ^{13}C-NMR spectra of **1**

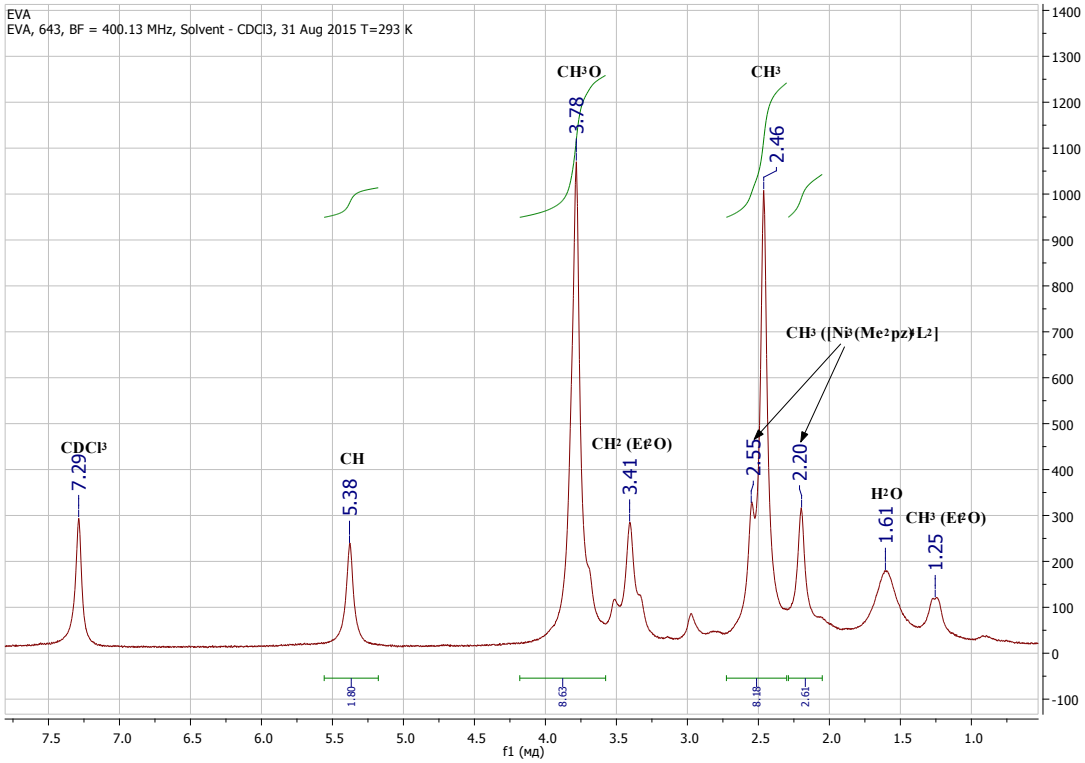

Figure S19. ^{1}H-NMR spectra of **2** and **4**

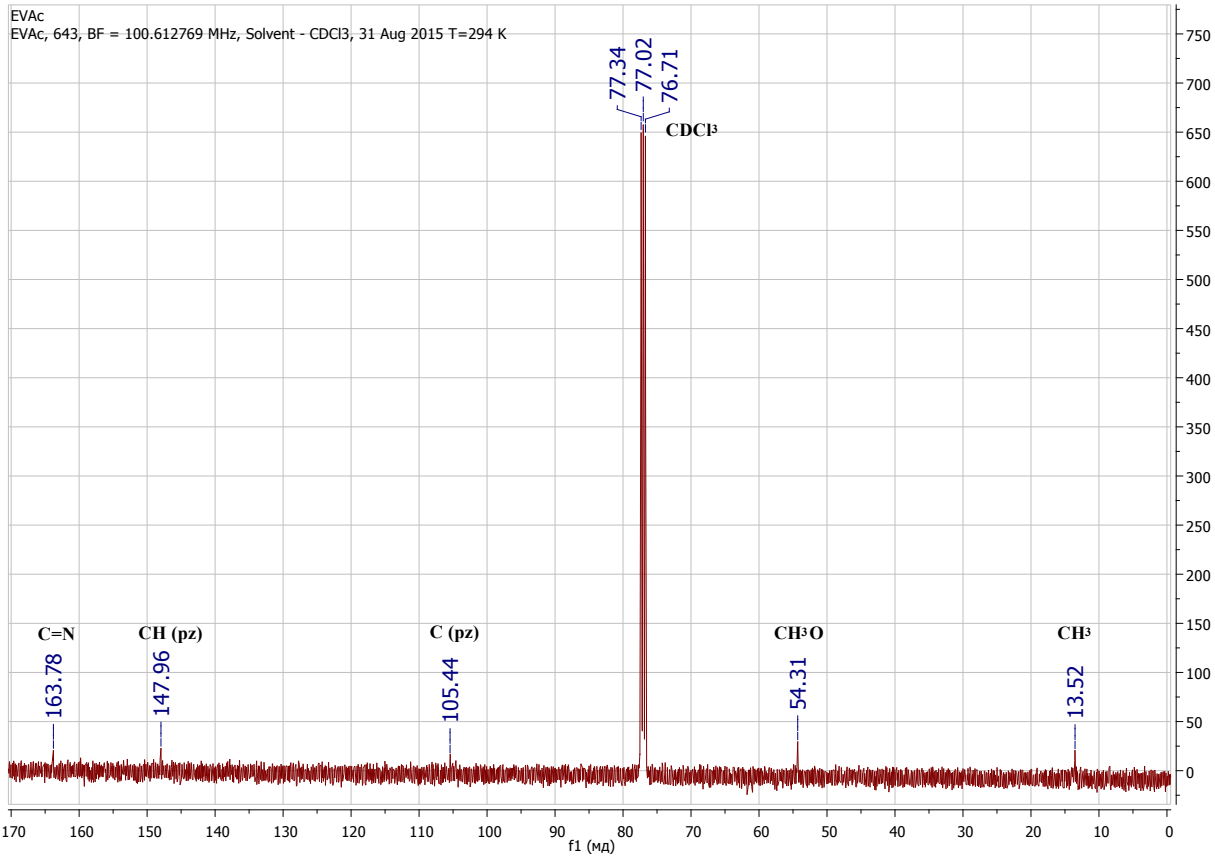

Figure S20. ^{13}C-NMR spectra of **2**

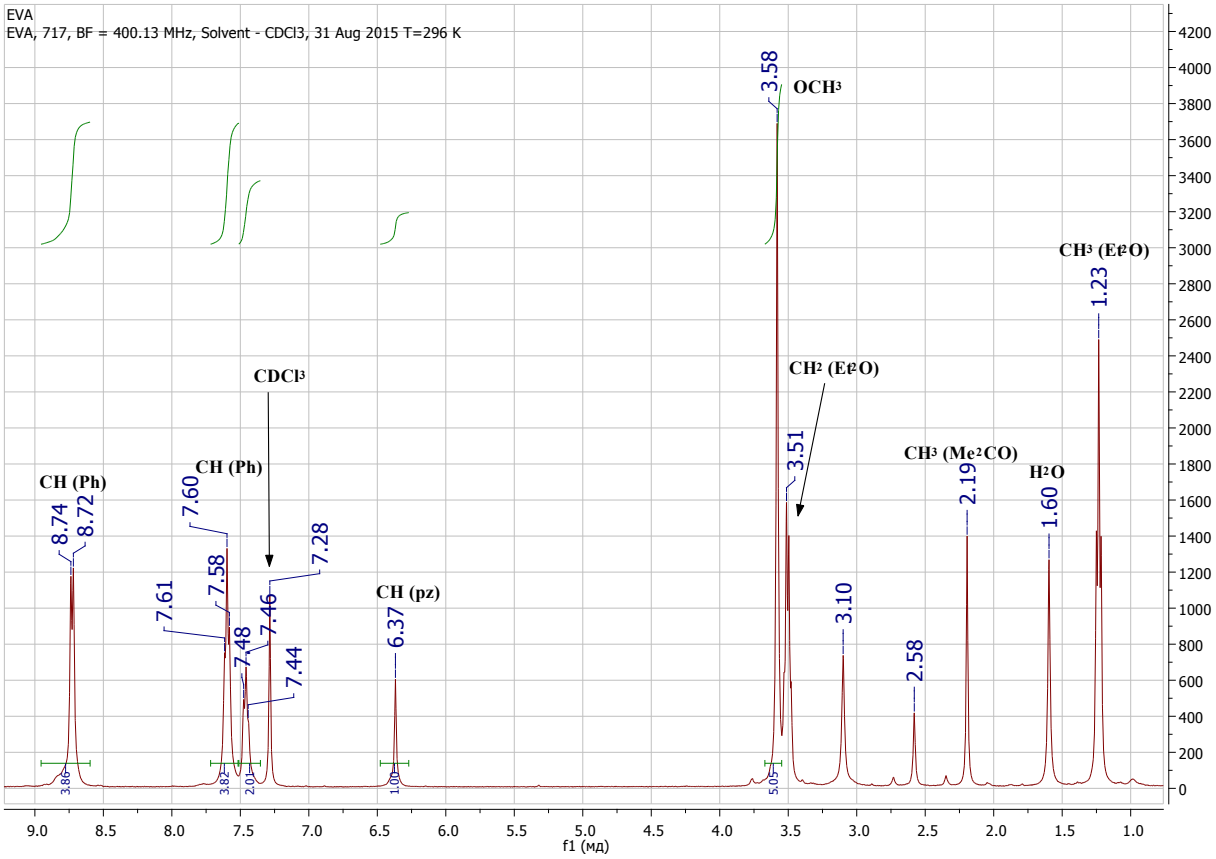

Figure S21. ^{1}H-NMR spectra of **3**

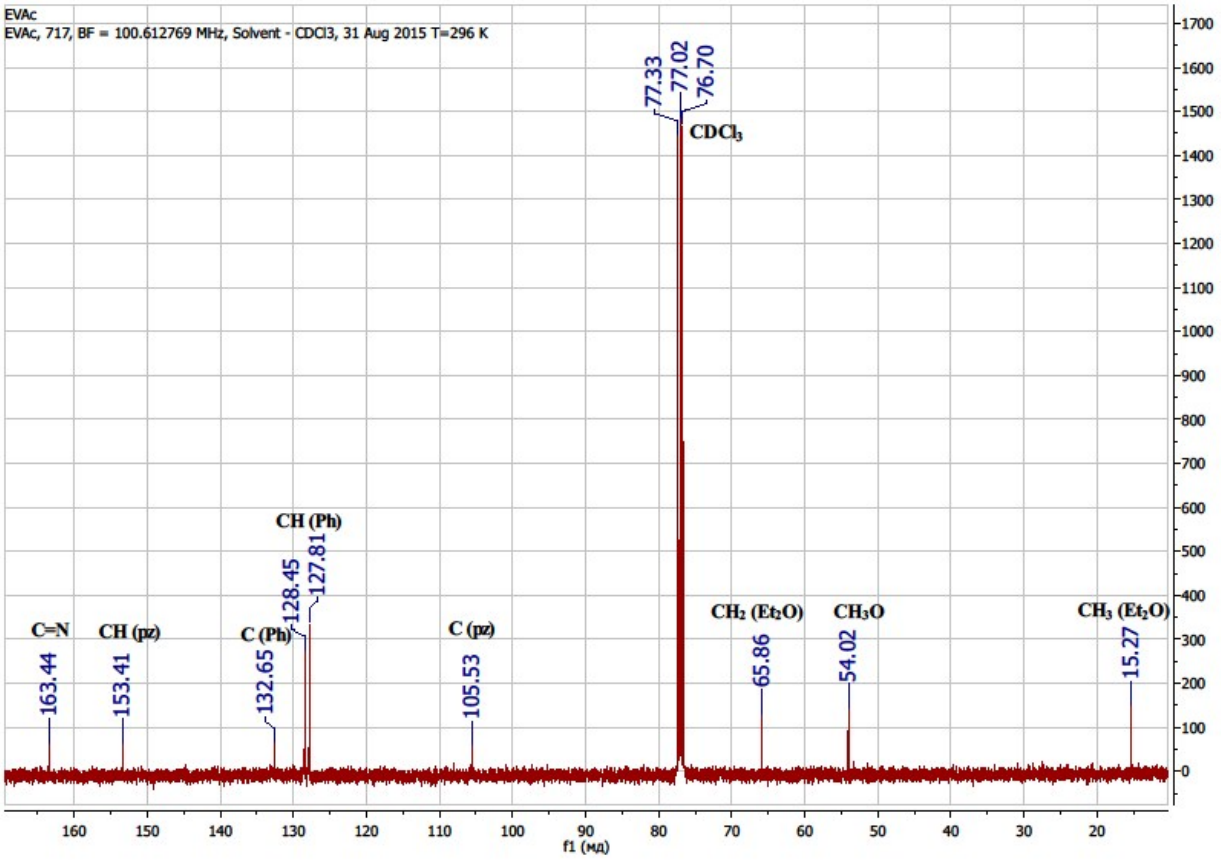

Figure S22. ^{13}C-NMR spectra of **3**

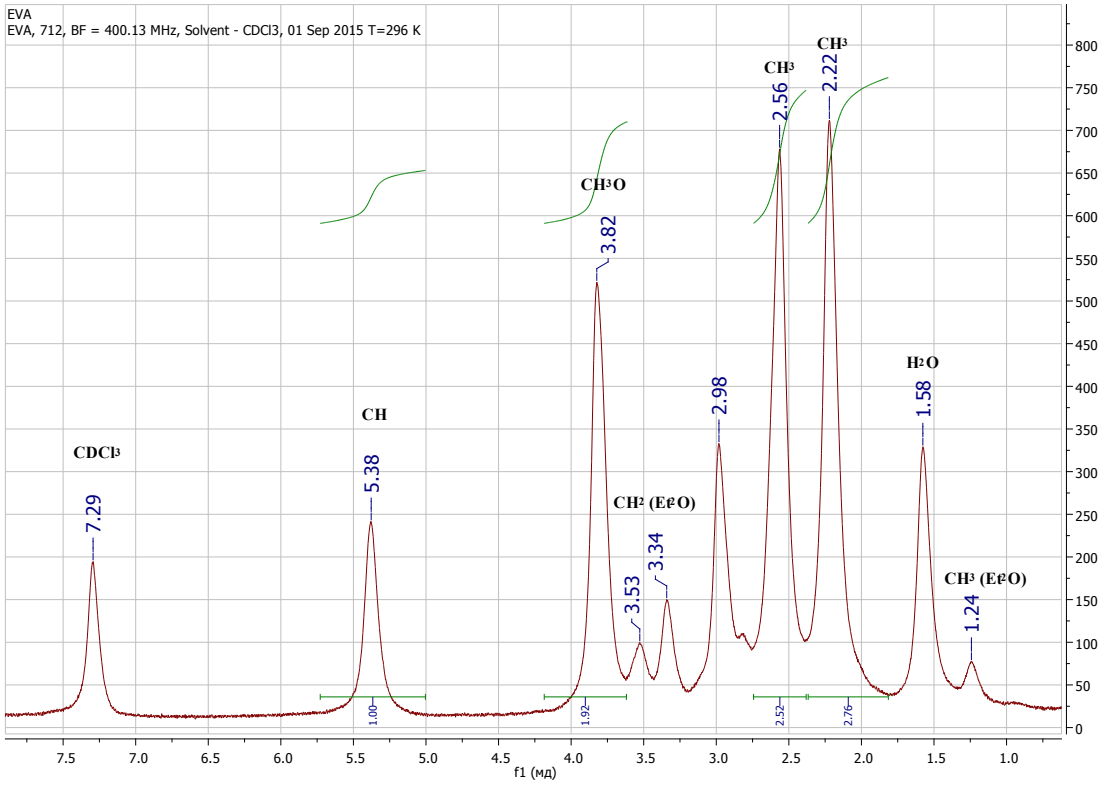

Figure S23. ^{1}H-NMR spectra of **4**

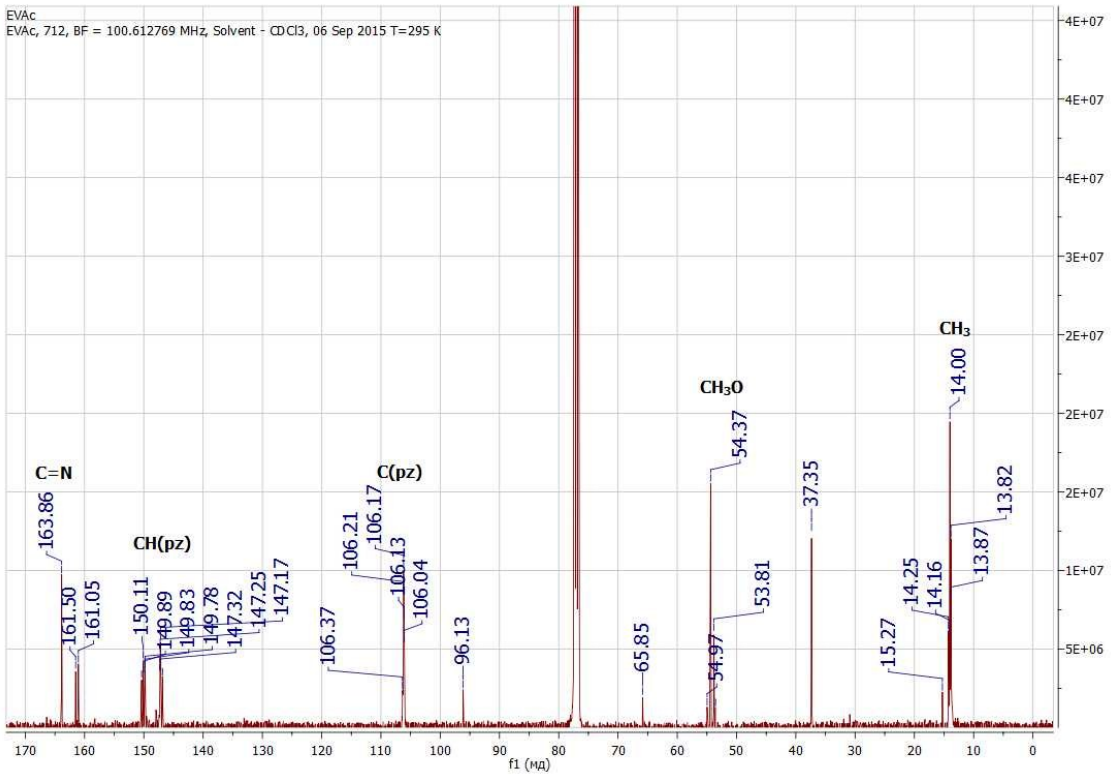

Figure S24. ^{13}C-NMR spectra of **4**

Powder XRD data for reaction mixtures

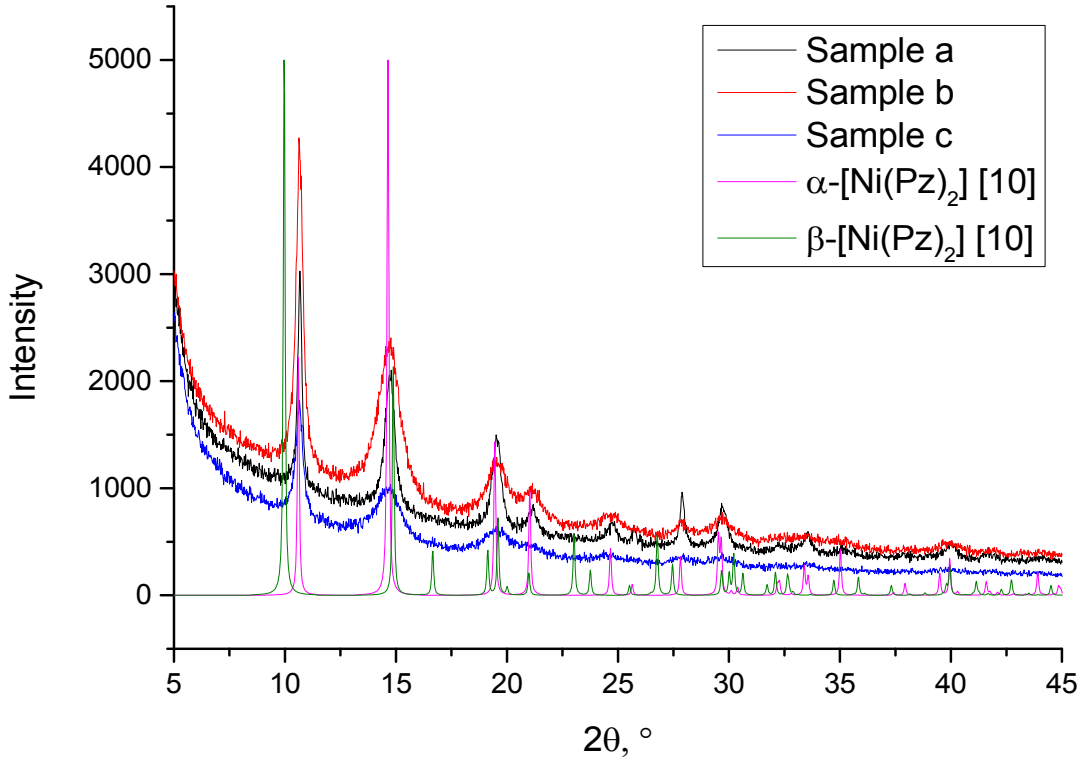

Figure S25. Powder XRD for the products of reaction NiX_2 with PzH in MeOH. The samples were obtained from the systems $NiX_2/NCNR_2/PzH$: at 1/1/2 (a), 1/2/4 (b), 1/6/2 (c) molar ratios.

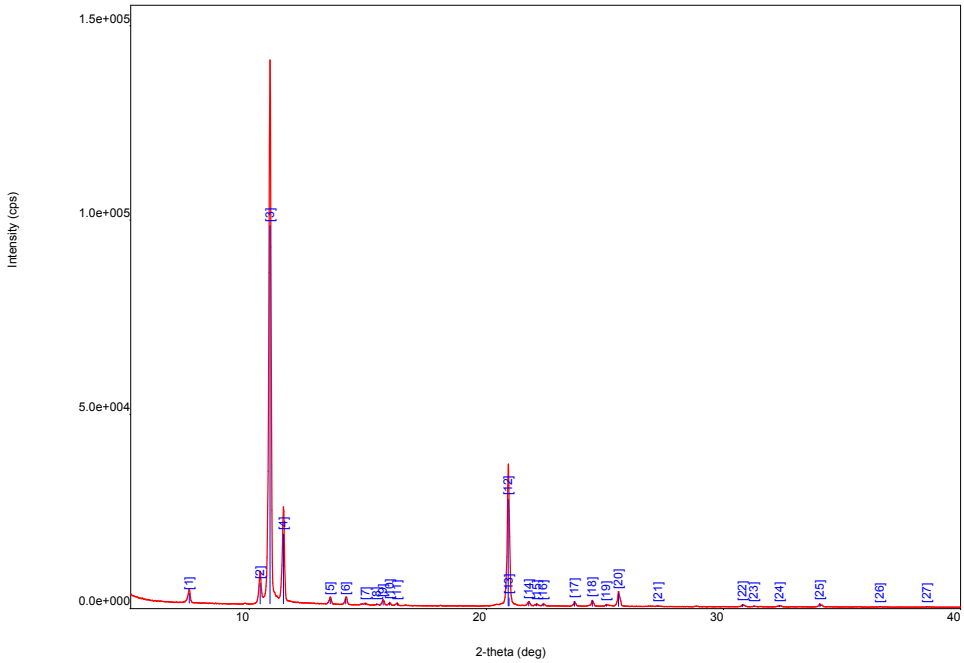

Figure S26. Powder XRD for the product of reaction complex **1** and $NiCl_2$ with Me_2PzH in MeOH

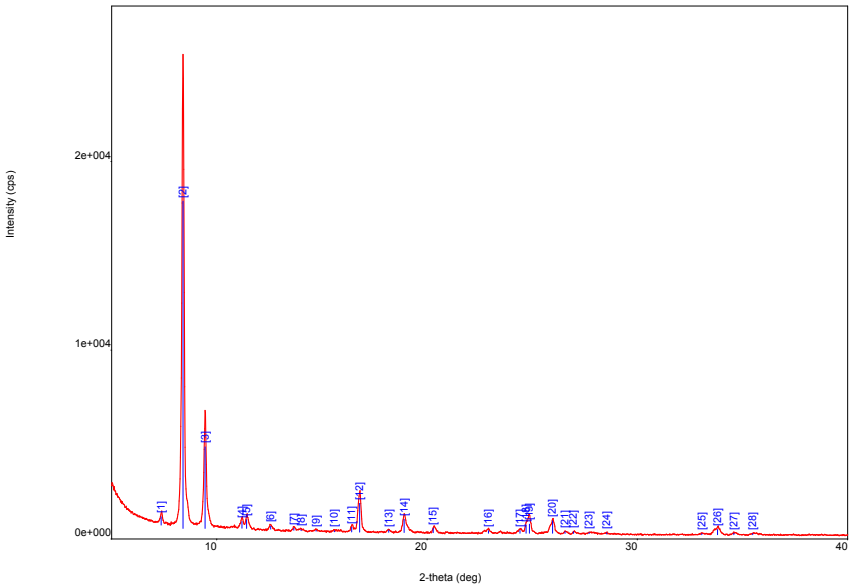

Figure S27. Powder XRD for the product of reaction complex **2** and $NiCl_2$ with Me_2PzH in DMF

Thermogravimetric data for complexes 1–4

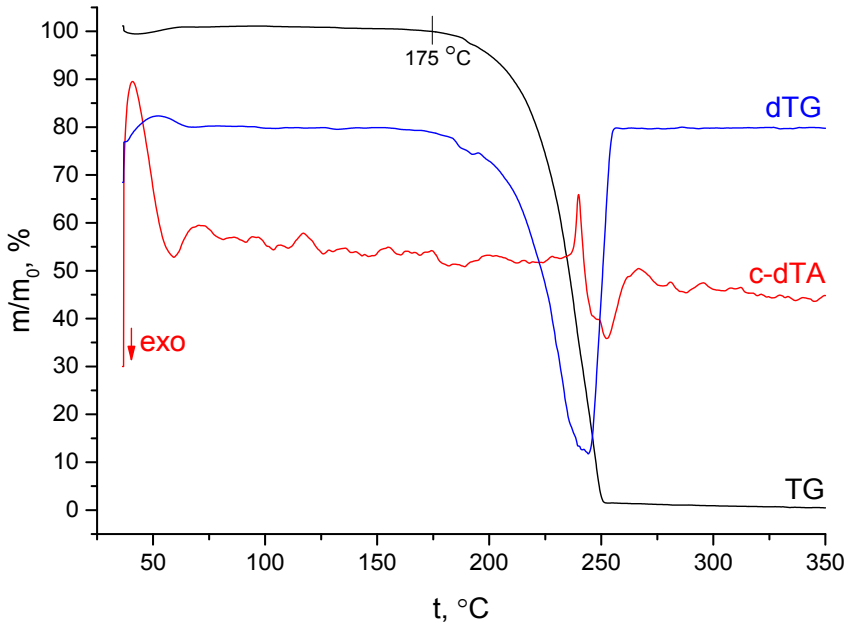

Figure S28. TG, dTG and c-DTA curves for the thermal decomposition of **1**

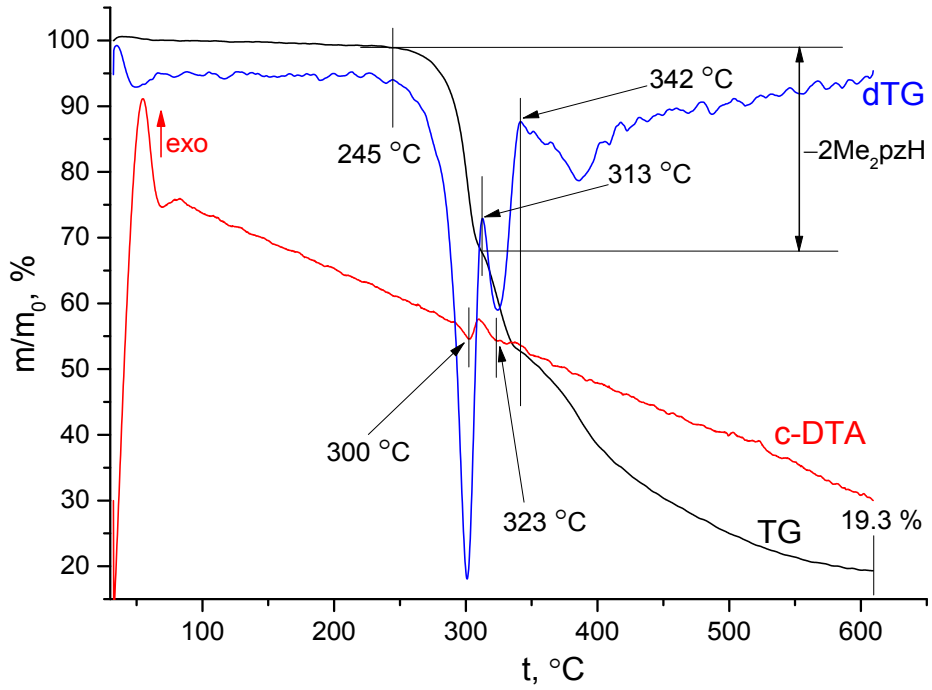

Figure S29. TG, dTG and c-DTA curves for the thermal decomposition of **2**

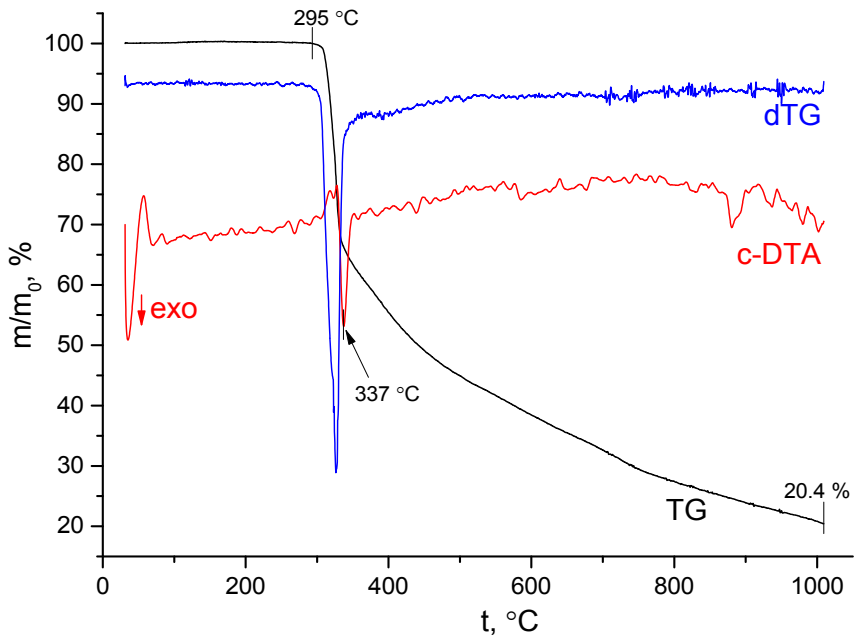

Figure S30. TG, dTG and c-DTA curves for the thermal decomposition of **3**

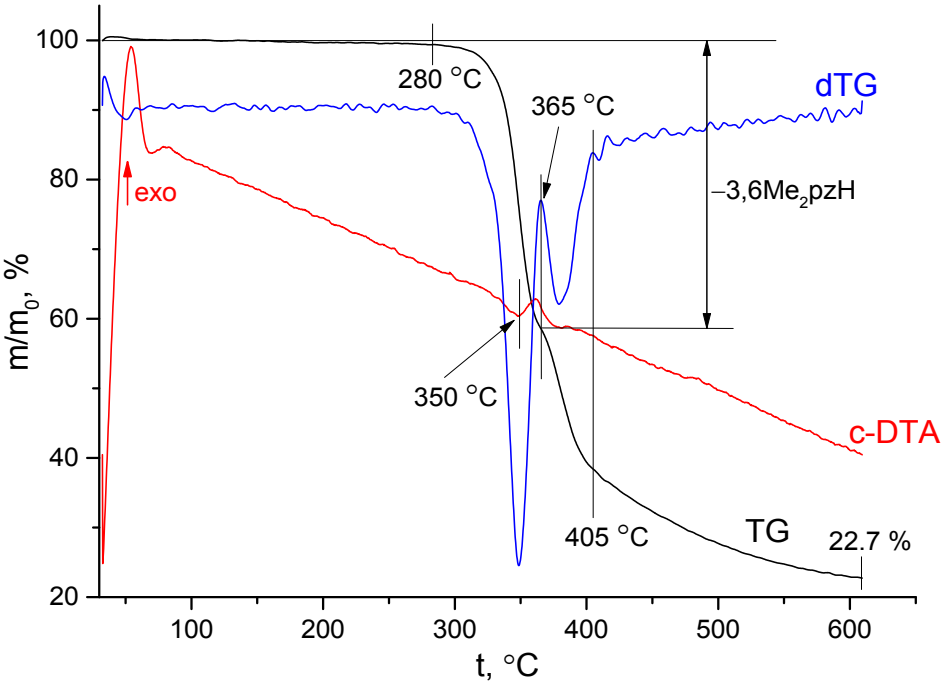

Figure S31. TG, dTG and c-DTA curves for the thermal decomposition of **4**

References

1. E. V. Andrusenko, N. A. Bokach, G. L. Starova and V. Y. Kukushkin, *Inorg. Chim. Acta*, 2014, **423**, 307-312.
2. Q.-Q. Wang, R. A. Begum, V. W. Day and K. Bowman-James, *Org. Biomol. Chem.*, 2012, **10**, 8786 – 8793.
3. a) J.-m. Huang, C. Qian, L. Feng, Y.-b. Chen and X.-z. Chen, *Monatsh. Chem.*, 2013, **144**, 1187-1190; b) V. N. Tsarev, Y. Morioka, J. Caner, Q. Wang, R. Ushimaru, A. Kudo, H. Naka and S. Saito, *Org. Lett.*, 2015, **17**, 2530-2533; c) L. Zhang, Y. Zhang, Y. Deng and F. Shi, *RSC Adv.*, 2015, **5**, 14514-14521.
4. a) T. T. Dang, B. Ramalingam and A. M. Seayad, *ACS Catal.*, 2015, **5**, 4082-4088; b) F. Li, J. Xie, H. Shan, C. Sun and L. Chen, *RSC Adv.*, 2012, **2**, 8645-8652.
5. a) K.-I. Watanabe and K. Sakai, *Bull. Chem. Soc. Japan*, 1966, **39**, 8–14; b) K.-I. Watanabe, *Bull. Chem. Soc. Japan*, 1964, **37**, 1325-1329.
6. J. Borau-Garcia, D. V. Gutsulyak, R. J. Burforda and W. E. Piers, *Dalton Trans.*, 2015, **44**, 12082-12085.
7. T. Bolano, T. B. Gunnoe and M. Sabat, *Dalton Trans*, 2013, **42**, 347-350.
8. a) WO2009106237A2, 2009; b) L. Dou, X. Zhao, H. An, G. Wang and Y. Wang, *Ind. Eng. Chem. Res.*, 2013, **52**, 4408-4413; c) X. Guo, J. Shang, J. Li, L. Wang, Y. Ma, F. Shi and Y. Deng, *Synth. Commun.*, 2011, **41**, 1102-1111; d) S. P. Rannard, N. J. Davis and I. Herbert, *Macromolecules*, 2004, **37**, 9418-9430; e) M. Wang, H. Wang, N. Zhao, W. Wei and Y. Sun, *Catal. Commun.*, 2006, **7**, 6-10; f) M. Wang, N. Zhao, W. Wei and Y. Sun, *Ind. Eng. Chem. Res.*, 2005, **44**, 7596-7599.
9. a) Y. Tsuji, R. Takeuchi, H. Ogawa and Y. Watanabe, *Chem. Lett.*, 1986, 293–294; b) G. Guillena, D. J. Ramon and M. Yus *Chem. Rev.*, 2010, **110**, 1611–1641.
10. a) M. N. Kopylovich, A. M. Kirillov, E. A. Tronova, M. Haukka, V. Y. Kukushkin and A. J. L. Pombeiro, *Eur. J. Inorg. Chem.*, 2010, **2010**, 2425-2432; b) N. Heße, R. Fröhlich, I. Humelnicu and E.-U. Würthwein, *Eur. J. Inorg. Chem.*, 2005, **11**, 2189–2197; c) P. V. Gushchin, K. V. Luzyanin, M. N. Kopylovich, M. Haukka, A. J. L. Pombeiro and V. Y. Kukushkin, *Inorg. Chem.*, 2008, **47**, 3088-3094.
11. a) M.-L. Tong, Y.-M. Wu, Y.-X. Tong, X.-M. Chen, H.-C. Chang and S. Kitagawa, *European Journal of Inorg. Chem.*, 2003, **2003**, 2385-2388; b) R. Boca, M. Hvastijova and J. Kozisek, *J. Chem. Soc., Dalton Trans.*, 1995, 1921-1923.
12. I. M. Atkinson, M. M. Bishop, L. F. Lindoy, S. Mahadev and P. Turner, *Chem. Commun. (Cambridge, U. K.)*, 2002, DOI: 10.1039/b206898b, 2818-2819.
13. a) N. Q. Shixaliyev, A. M. Maharramov, A. V. Gurbanov, N. V. Gurbanova, V. G. Nenajdenko, V. M. Muzalevskiy, K. T. Mahmudov and M. N. Kopylovich, *J. Mol. Struct.* 2013, **1041**, 213–218; b) M. M. Bishop, L. F. Lindoy, B. W. Skelton and A. H. White, *J. Chem. Soc., Dalton Trans.*, 2002, DOI: 10.1039/b108070a, 377–382; c) M. Zhu, L. Lu, P. Yanga and X. Jin, *Acta Cryst. Sect. E*, **E58**, m272–m274.
14. a) S. J. Rettig, A. Storr, D. A. Summers, R. C. Thompson and J. Trotter, *Canadian J. Chem.*, 1997, **75**, 949-958; b) K. Fujita, S. Hikichi, M. Akita and Y. Moro-oka, *J. Chem. Soc., Dalton Trans.*, 2000, DOI: 10.1039/A908181J, 117-119; c) P. J. Altmann and A. Pöthig, *Chem. Comm.*, 2016, DOI: 10.1039/C6CC00507A, 9089–9092; d) K. S. Chong, S. J. Rettig, A. Storr and J. Trotter, *Canadian J. Chem.*, 1979, **57**, 3090-3098.
15. a) M. Maekawa, M. Munakata, T. Kuroda and Y. Nozaka, *Inorg. Chim. Acta*, 1993, **208**, 243-244; b) S. J. R. Kenneth S. Chong, Alan Storr, James Trotter, *Canadian J. Chem.*, 1981, **59**, 996-1006.
16. R. F. W. Bader, *Atoms in Molecules: A Quantum Theory*, Oxford University Press, Oxford, 1990.

17. S. Alvarez, A cartography of the van der Waals territories, *Dalton Trans*. 2013, **42**, 8617–8636; 10.1039/c3dt50599e
18. R. F. W. Bader, Atoms in Molecules: A Quantum Theory, Oxford University Press, Oxford, 1990.
19. E. Espinosa, E. Molins and C. Lecomte, *Chem. Phys. Lett.*, 1998, **285**, 170–173.
20. M. V. Vener, A. N. Egorova, A. V. Churakov and V. G. Tsirelson, *J. Comput. Chem.* 2012, **33**, 2303-2309.
21. E. Espinosa, I. Alkorta, J. Elguero and E. Molins From weak to strong interactions: A comprehensive analysis of the topological and energetic properties of the electron density distribution involving X–H···F–Y systems, *J. Chem. Phys.*, 2002, **117**, 5529−5542; 10.1063/1.1501133.